Università degli Studi di Padova

Master Thesis

Satellite Channel Impairments: link performace degradation and countermeasures

Author:
Luca Barbiero

Supervisor:
Prof. Andrea Galtarossa
Dr. Eros Feltrin

A thesis submitted in fulfilment of the requirements
for the degree of Laurea Magistrale in Ingegneria delle Telecomunicazioni

in the

Department of Information Engineering

June 2014

UNIVERSITÀ DEGLI STUDI DI PADOVA

Abstract

School of Engineering
Department of Information Engineering

Laurea Magistrale in Ingegneria delle Telecomunicazioni

Satellite Channel Impairments: link performace degradation and countermeasures

by Luca Barbiero

The world of geo-synchronous satellite communications is witnessing for several months now, a strong discussion, if not a dispute, between some system manufacturers about the oppurtunity of increasing the efficiency of the coding schemes proposed by the second generation of the Digital Video Broadcasting standard by introducing some extensions. Even if the debate rises the interest of operators and manufacturers, its conclusions are far from being unanimously accepted. The reason for this is that the benefits of such extensions are yet not clear in practical satellite channels, where impairments like non-linearities, group delay variations, adjacent channel interference and phase noise negatively impact the end-to-end link performance. These must be carefully taken into account, since they put limits in terms of spectral efficiency achievable for a certain system architecture and link budget. This work seeks to quantify the effect of such impairments under both single carrier and multi-carrier per transponder scenarios, with a particular attention to the implications of sharper filters Roll-Offs. Further, the benefits of countermeasures such as waveform pre-distortion, post-compensation techniques and high power amplifier linearisation are also analysed and compared for different system configurations. The results achieved here have been obtained jointly by computer simulations and lab measures carried out in the Teleport of Eutelsat Communications, in collaboration with the department of Multimedia and Added Value Services.

Acknowledgements

I would like to thank my professors of the Department of Information Engineering for the high quality teaching they gave me, and in particular Professor Andrea Galtarossa for endorsing me at Eutelsat Communications. This thesis work, which I carried out in the facilities of the company, was only possible thanks to the Department of Multimedia and Added Value Services of Eutelsat. I would like to express sincere gratidute to my project advisor Eros Feltrin for the opportunity of working with him and his colleagues, and to all the staff of the department for the reception I received. A special thanks goes to Antoine Bonnaud for his continuos support.

Contents

List of Figures

List of Tables

Ai miei genitori, che mi hanno sempre sostenuto in questo lungo cammino

Chapter 1

Introduction

1.1 Satellite Communication Systems

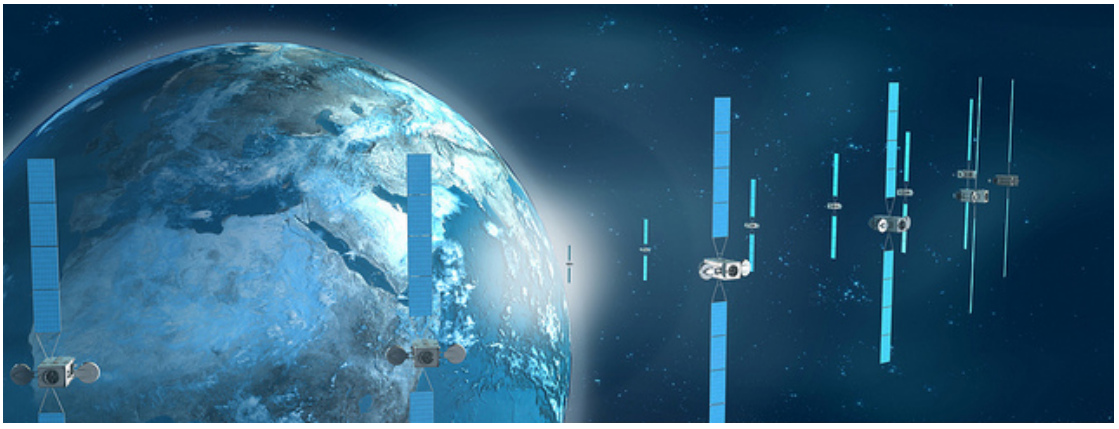

Satellite communications are the outcome of research in the area of both communications and aerospace, and arise from the expertise gained in two very different areas - missiles and microwaves - during the Second World War. The whole space era started in 1957 with the launch of the first artificial satellite (Sputnik). During the sixties the first commercial geostationary satellites were launched, opening *de facto* an ever growing evolution of services which still continues today. Originally these were designed to carry communications from one point to another, as with cables, and the extended coverage of the satellite was used to set up long distance links (for example connecting stations on the two opposite sides of the Atlantic Ocean, Early Bird 1965). The increasing size and power of satellites permitted a consequent reduction in the size of earth stations, and hence their cost, leading to an increase in number. In this way it has been possible to exploit another feature of the satellite which is its ability to collect or broadcast signals from or to several locations. Instead of transmitting signals from one point to another, transmission can be from a single transmitter to a large number of receivers distributed

over a wide area or, conversely, transmission can be from a large number of stations to a single central station, often called a hub. In this way, multipoint data transmission networks and data collection networks have been developed under the name of VSAT (very small aperture terminals) networks. For TV services, satellites are of paramount importance for broadcasting, news gathering, exchange of programmes between broadcasters, and in general for distributing programmes to terrestrial broadcasting stations and cable heads, or directly to the individual consumer. The latter are commonly called direct broadcasting by satellite (DBS) systems, or direct-to-home (DTH) systems. These operate with small earth stations having antennas with a diameter from 0.5 to 1 m. In the past, the customer stations were *receive only* stations.

With the introduction of two-way communications stations, satellites became a key component in providing interactive TV and broadband Internet services thanks to the implementation of the satellite return channel to the service providers facilities. This uses TCP/IP to support Internet, multicast and web-page caching services over satellite with forward channel operating at several Mbit/s and enables satellites to provide broadband service applications for the end user, such as direct access and distribution services. IP-based triple-play services (telephony, Internet and TV) has become more and more popular, after the introduction of the DVB-S2. Satellite based systems cannot compete with terrestrial Asymmetric Digital Subscriber Line (ADSL) or cable to deliver these services in high-density population areas. However, they complement nicely the terrestrial networks around cities and in rural areas when the distance to the telephone

router is too large to allow delivery of the several Mbit/s required to run the service [1]. A typical satellite system is composed of:

- the *space segment* containing one or more satellites organised into a constellation,
- the *control segment* containing all the ground facilities for control and monitoring of the satellites,
- the *ground segment* containing the traffic earth stations.

Traffic earth stations come in three classes: *user stations*, such as handsets, portables, mobile stations and very small aperture terminals (VSATs), which allow the customer direct access to the space segment; *interface stations*, known as gateways, which interconnect the space segment to a terrestrial network; and *service stations*, such as hub or feeder stations, which collect or distribute information from and to user stations via the space segment. The path from a source user terminal to a destination user terminal is named a simplex connection.

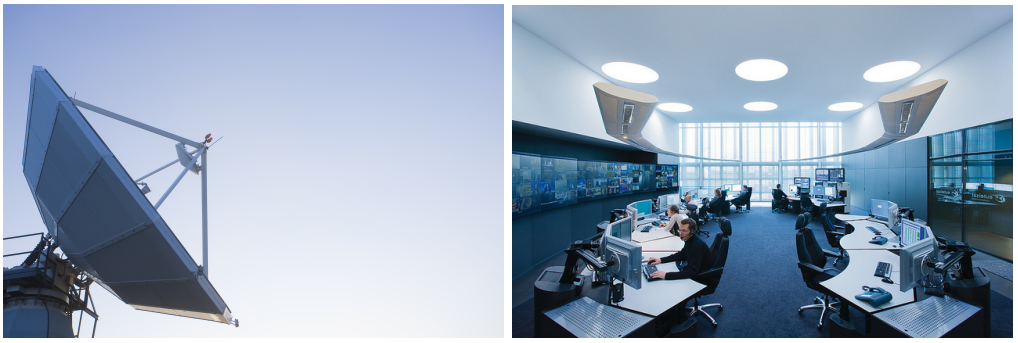

FIGURE 1.1: A modern Satellite Teleport.

There are two basic schemes: single connection per carrier (SCPC), where the modulated carrier supports one connection only, and multiple connections per carrier (MCPC), where the modulated carrier supports several time or frequency multiplexed connections. Interactivity between two users requires a duplex connection between their respective terminals, i.e. two simplex connections, each along one direction. Each user terminal should then be capable of sending and receiving information. A connection between a service provider and a user goes through a hub (for collecting services) or a feeder station (e.g. for broadcasting services). A connection from a gateway, hub or feeder station to a user terminal is called a forward connection. The reverse connection is the return connection. Both forward and return connections entail an uplink (from earth station to the satellites), a downlink (from the satellites to the earth stations), and possibly one or more inter-satellite links (between the satellites) [1].

The link performance can be measured by the ratio of the received carrier power C, to the noise power N, and is denoted as the C/N ratio. The values of C/N, for the links which participate in the connection between the end terminals, determine the quality of service, specified for digital communications in terms of bit error rate (BER) or packet error rate (PER). Another parameter of importance for the design of a link is the bandwidth, B, occupied by the carrier. This bandwidth depends on the information data rate, the channel coding rate (forward error correction) and the type of modulation used to modulate the carrier. For a target information rate, the trade-off between required carrier power and occupied bandwidth is paramount to the cost-effective design of the link. This is an important aspect of satellite communications as power impacts both satellite mass and earth station size, and bandwidth is constrained by regulations.

1.2 The Space Segment

The satellite as a spacecraft is made of the payload and the platform. The payload consists of the receiving and transmitting antennas and all the electronic equipment which supports the transmission of the carriers, while the platform supports and accommodate the payload in the space environment. The payload can act as either a transparent or regenerative repeater. It can be shown that regenerative repeaters can achieve better link performance and hence better quality of service, however in practice transparent repeaters are often preferred because of their simplicity (i.e. lower cost) and higher flexibility (being system independent) . In a transparent payload the carrier power is amplified and frequency is downconverted. Power gain is of the order of 100 to 130 dB, required to raise the power level of the received carrier from a few tens of picowatts to the power level of the carrier fed to the transmit antenna of a few watts to a few tens of watts. Frequency conversion is required to increase isolation between the receiving input and the transmitting output. Due to technology power limitations, the overall satellite payload bandwidth is split into several sub-bands, the carriers in each sub-band being amplified by a dedicated power amplifier. This is mainly to combat the intermodulation phenomenon, as we shall see in detail in Chapter 4. The amplifying chain associated with each sub-band is called a satellite channel, or transponder. The bandwidth splitting is achieved using a set of filters called the input multiplexer (IMUX). The amplified carriers are recombined in the output multiplexer (OMUX). Later on we will refer to IMUX and OMUX as well for a specific pair of input and output filters. The High Power Amplifiers (HPAs) associated with each transponder are typically driven close to saturation, in order to exploit as much as possible the available power in the downlink. However this makes the satellite channel non-linear, and introduces some distortion on the transmitted waveform, as we will discuss in detail in Chapter 2.

1.3 The DVB-S2 Standard and the new DVB-S2X extensions

Standardization plays a fundamental role in the spread of communication technologies. In fact standardization

- encourages innovation,
- fosters enterprise opening new markets,
- creates trust and confidence in products,
- brings down costs and increases competition,
- helps preventing the duplication of effort.

The Digital Video Broadcasting (DVB) is a suite of internationally accepted open standards for digital television. DVB standards are developed and maintained by the DVB Project, an international industry consortium with more than 200 members in Europe and worldwide. The specifications developed by the DVB Project are passed to the European Telecommunications Standards Institute for approval. The DVB-S system for digital satellite broadcasting was developed in 1993. It is a relatively straightforward system using QPSK and convolutional forward error correction (FEC), concatenated with ReedSolomon coding. The tools for channel coding and error protection introduced in its specifications were used later on for other delivery media systems. DVB-S links also started to be proposed for professional point-to-point transmission of television programs, to convey directly to the broadcasters premises audio/video material originated in the studios (TV contribution) and/or from remote locations by outside broadcasting vans or portable uplink terminals, without requiring a local access to the fixed telecom network (Digital Satellite News Gathering). In 1998, DVB produced its second standard for satellite applications, DVB-DSNG, extending the functionalities of DVB-S to include higher order modulations (8PSK and 16QAM) for DSNG and other TV contribution applications by satellite.

The results of this evolutionary trend, together with the increase in the operators and consumers demand for larger capacity and innovative services by satellite, led the DVB Project to define in 2003 the second-generation system for satellite broad-band services, DVB-S2. The system has been designed for different types of applications:

- broadcasting of standard definition and high-definition TV (SDTV and HDTV);
- interactive Services, including Internet access, for consumer applications (for integrated receiversdecoders (IRDs) and personal computers);
- professional applications, such as digital TV contribution and news gathering;
- data content distribution and Internet trunking.

To be able to cover all these application areas while still keeping the single-chip decoder at reasonable complexity levels, DVB-S2 is structured as a *toolkit*, thus also enabling the use of mass market products for professional or niche applications. The DVB-S2 standard has been specified around three key concepts: best transmission performance, total flexibility, and reasonable receiver complexity. To achieve the best performance-complexity trade-off, quantifiable in about 30% capacity gain over DVB-S, DVB-S2 benefits from more recent developments in channel coding and modulation. For interactive point-to-point applications such as IP unicasting, the adoption of the adaptive coding and modulation (ACM) functionality allows optimization of the transmission parameters for each individual user on a frame-by-frame basis, dependent on path conditions, under closed-loop control via a return channel (connecting the IRD/PC to the DVB-S2 uplink station via terrestrial or satellite links, signaling the IRD/PC reception condition). This results in a further increase in the spectrum utilization efficiency of DVB-S2 over DVB-S, allowing the optimization of the space segment design, thus making possible a drastic reduction in the cost of satellite-based IP services. DVB-S2 is so flexible that it can cope with any existing satellite transponder characteristics, with a large variety of spectrum efficiencies and associated C/N requirements. Furthermore it is designed to handle a variety of advanced audiovideo formats which the DVB Project defined. DVB-S2 accommodates any input stream format, including single or multiple MPEG transport streams (TSs) (characterized by 188-byte packets), IP as well as ATM packets and continuous bit-streams.

1.3.1 DVB-S2 System architecture

The DVB-S2 transmission system is structured as a se- quence of functional blocks, schematically represented in Figure 1.3. Signal generation is based on two levels of framing structures:

- BBFRAME at base-band (BB) level, carrying a variety of signaling bits, to configure the receiver flexibly ac- cording to the application scenario.

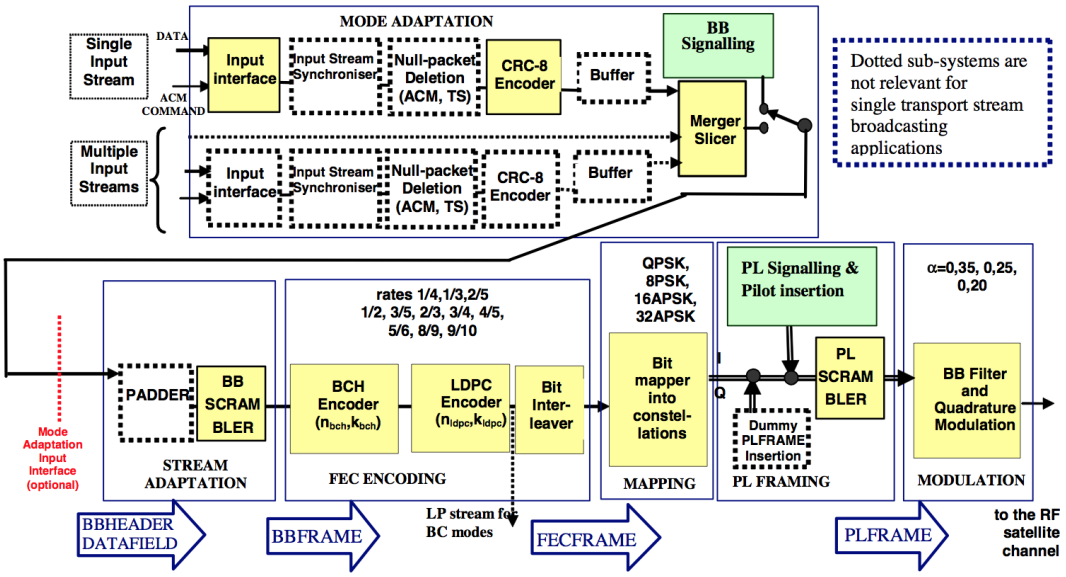

FIGURE 1.3: Functional block diagram of the DVB-S2 system.

- PLFRAME at physical layer (PL) level, carrying few highly protected signaling bits, to provide robust syn- chronization and signaling at the physical layer.

Depending on the application, DVB-S2 input sequences may be single or multiple MPEG TSs, single or multiple generic streams, either packetized or continuous. Mode and stream adaptation blocks provide input stream interfacing, synchronization, and other optional tools. Furthermore, for multiple inputs, it provides merging of input streams in a single transmission signal and slicing in FEC code blocks (identified as data blocks), composed of bits taken from a single input port, to be transmitted in a homogeneous transmission mode (FEC code and modulation). Then baseband frames BBFRAME are built by appending the base-band header (80 bits) in front of the data block, to notify the receiver of the input stream format and Mode Adaptation type: single or multiple input streams, generic or TS, constant coding and modulation (CCM) or adaptive coding and modulation (ACM), and many other configuration details. Thanks to the FEC protection (covering both the header and the data payload) and the wide length of the FEC frame, the base-band header can in fact contain many signaling bits without losing transmission efficiency or ruggedness against noise. In case the user data available for transmission are not sufficient to completely fill a BBFRAME, padding bits are also inserted to complete it. Finally, base-band scrambling is performed.

The Forward Error Correction (FEC) subsystem relies on the concatenation of outher BCH and inner irregular LDPC codes, and is key to achieve excellent performance by satellite, in the presence of high levels of noise and interference. The total BCH+LDPC block length is 64800 bits for applications not too critical for delays, 16200 bits otherwise. Code rates of 1/4, 1/3, 2/5, 1/2, 3/5, 2/3, 3/4, 4/5, 5/6, 8/9, and 9/10 are available

depending on the selected constellation and the system application. In particular, coding rates 1/4, 1/3, and 2/5 have been introduced to operate, in combination with QPSK, under exceptionally poor link conditions, for signal to noise ratios below 0dB.

Error rate requirements for DVB-S2 are very stringent, 10^{-7} MPEG TS packet error rate (PER), approximately corresponding to *less than one erroneous packet per hour for a service bit rate of 5 Mb/s*. Figure 1.4 shows the excellent DVB-S2 FEC performance in the AWGN channel for various code rates and modulations, with FEC-coded blocks of 64800 bits and less than 50 decoding iterations in the receiver. Short code blocks generally give a slightly worse performance, due to the smaller frame dimension.

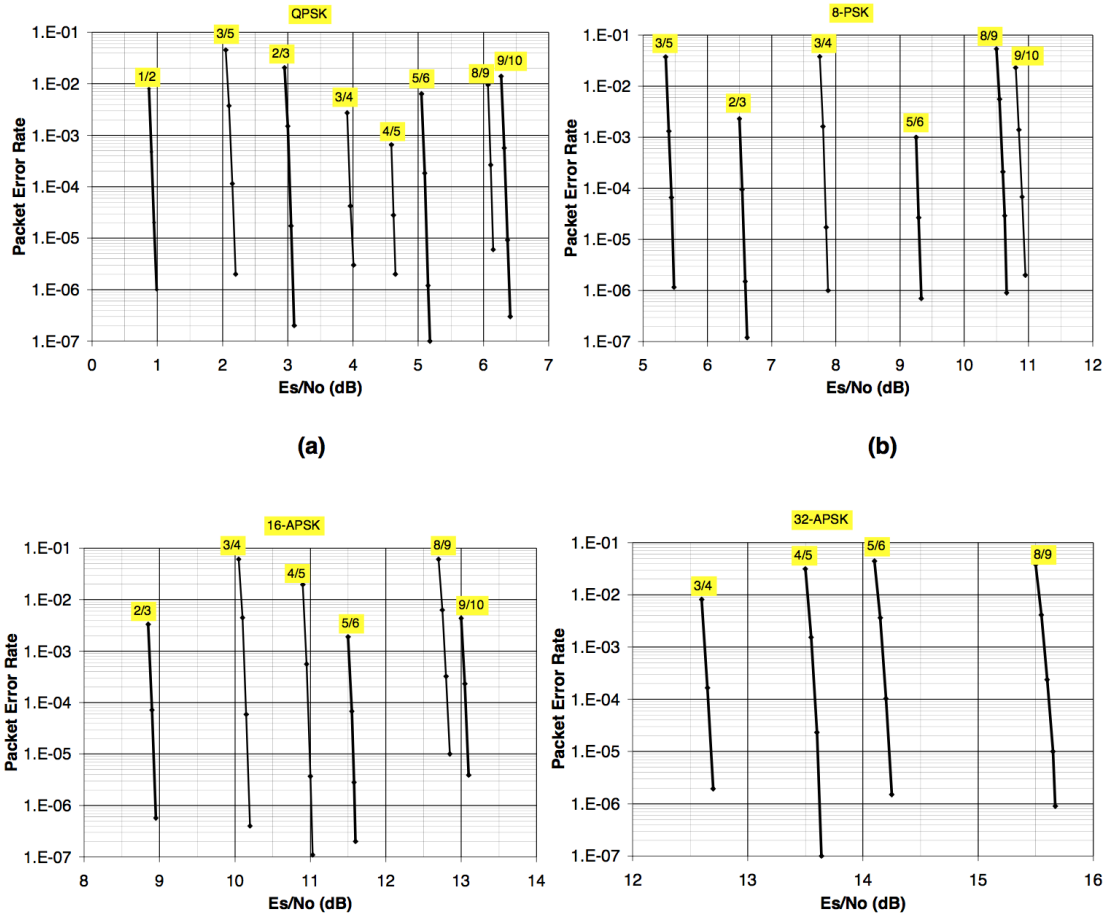

FIGURE 1.4: Performance of LDPC+BCH codes over AWGN channel. N = 64800 bits. (a) QPSK (b) 8PSK (c) 16APSK (d) 32APSK.

Four modulation modes can be selected for the transmitted payload (see Figure 1.5): QPSK, 8PSK, 16APSK, and 32APSK, depending on the application area. By selecting the modulation constellation and code rates, spectrum efficiencies from 0.5 to 4.5 bits per symbol are available and can be chosen dependent on the capabilities of the satellite transponder used. The 16APSK and 32APSK constellations have been op- timized for nonlinear transponders by placing the points on circles; nevertheless their performance

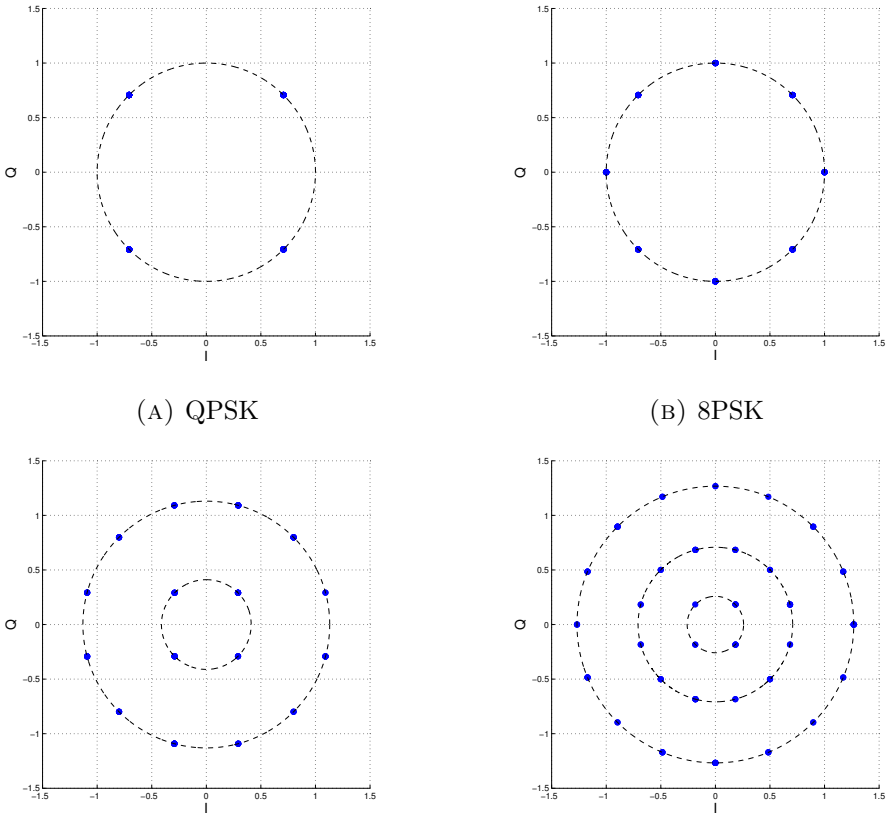

(A) QPSK (B) 8PSK

(C) 16APSK (D) 32APSK

FIGURE 1.5: The Four DVB-S2 symbol constellations.

in the AWGN channel is comparable with those of 16QAM or 32QAM respectively. QPSK and 8PSK are typically proposed for broadcast applications, since they are virtually constant envelope modu- lations and can be used in nonlinear satellite transponders driven near saturation. The 16APSK and 32APSK modes are mainly targeted at professional applications, due to the higher requirements in terms of available SNR, but they can also be used for broadcasting. While these modes are not as power efficient as the other modes, the spectrum efficiency is much greater. They need to operate the satellite transponder in a quasi-linear region or, alternatively, to adopt advanced predistortion methods in the uplink station to minimize the effect of transponder nonlinearity, as we shall se in Chapter 3.

The PL Framing subsystems accounts for the introduction of additional signalling symbols (such as the Start Of Frame sequence), optional dummy frame generation, pilot symbols insertion. The latter facilitate receiver synchronization. The DVB-S2 FEC codes are in fact so powerful that carrier recovery may become a serious problem for higher order modulations working at low SNRs in the presence of high levels of phase noise in consumer low noise block (LNB) converters and tuners: this is particularly the case with some low rate 8PSK, 16APSK, and 32APSK modes of DVB-S2. Pilots are

unmodulated symbols, identified by $I = Q = 1/\sqrt{2}$, grouped in blocks of 36 symbols and inserted every 16 payload slots, thus giving a maximum capacity loss of approximately 2.4% when used. Finally, scrambling for energy dispersal is carried out to comply with the Radio Regulations for spectrum occupancy and to transmit a sort of signature of the service operator, for a rapid identification in case of errors in the uplink procedures.

Square-root raised cosine baseband filtering and quadrature modulation are then applied, to shape the signal spectrum and to generate the RF signal. There are three permitted values for the rolloff factor: 0.35 as in DVB-S, plus 0.25 and 0.20 for tighter bandwidth restrictions (see also Appendix C).

1.3.2 DVB-S2X extensions

The satellite world has changed a lot since DVB-S2 was first published in 2005. Higher speeds, more efficient satellite communication technology and wider transponders are required to support the exchange of large and increasing volumes in data, video and voice over satellite. Moreover end-users expect to receive connectivity anywhere anytime they travel, live or work. The biggest demand for the extensions to the DVB-S2 standard

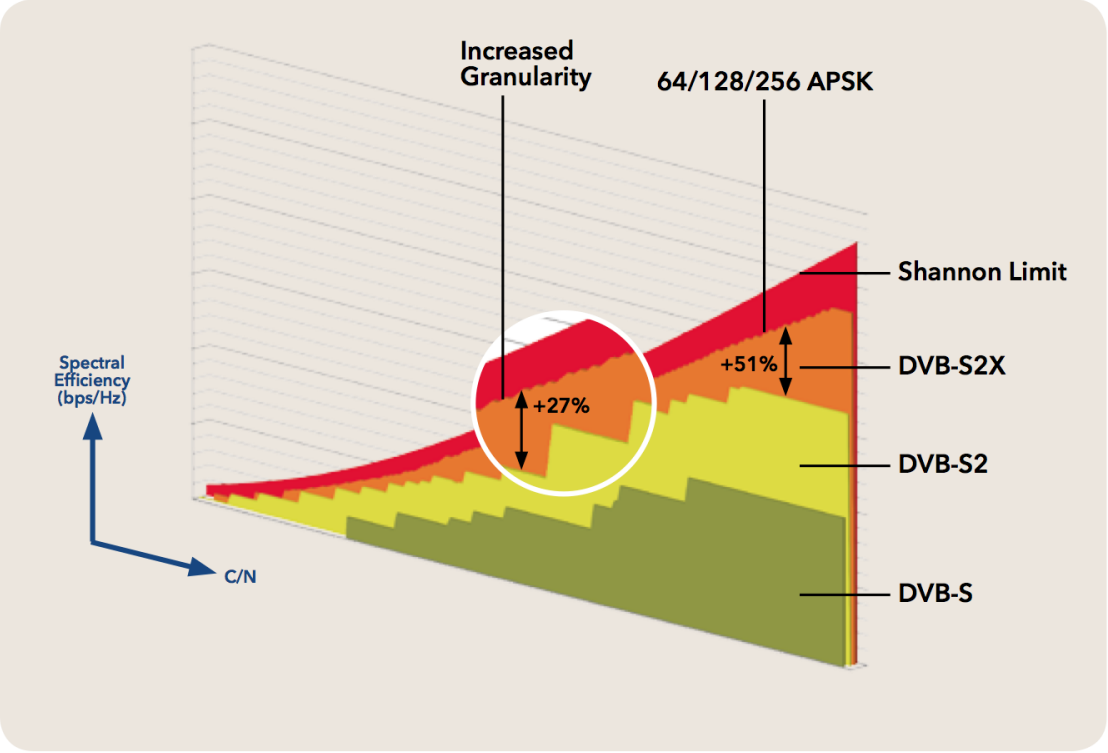

FIGURE 1.6: DVB-S2X compared to DVB-S2 (64/128/256APSK and increased granularity)

comes from video contribution and high-speed IP services, as these services are affected the most by the increased data rates.

In the long run more throughput will be required for Direct-to-Home applications as well with the rise of Ultra-High Definition TV (UHDTV) and the High Efficiency Video Coding (HEVC) video compression standard to support the request of higher quality images by the market. Ultimately, for satellite businesses, the creation and adoption of these extensions will translate to higher efficiency, higher speed, more mobility and greater service robustness to increase business and therefore revenues. The combination of technologies incorporated in the new standard results in a gain of up to 20% for DTH networks and 51% for other professional applications compared to DVB-S2 [2]. Many vendors, operators and satellite specialists within the industry did agree with DVB and have worked towards a new standard.

Hence, in March 2014, the DVB group released the DVB-S2X specifications [3]. The technologies involved in the new extension are:

- Low roll off, smaller carrier spacing and advanced filter technologies.
- MODCOD and FEC upgrades (including more granularity, adding 64, 128 and 256APSK)
- Wideband implementation.
- Very Low SNR MODCODs to support mobile (land, sea, air) applications.
- Bonding of TV streams.
- Additional standard scrambling sequences.

Figure 1.6 depicts the spectral efficiencies achieved by the DVB-S standard series, over the standard AWGN channel. The efficiency gain obtained by the DBV-S2X is remarkable especially for high SNRs, and non negligible in general. However, in practice channel impairments may significantly reduce such gain figures, and the introduction of higher order APSK constellations may turn out to be self defeating, for instance if the if the active components in the transmission chain exhibit a significant non-linear behavior. In the following, we present the results of a test campaign, which was carried out on available state of the art satellite modems, as well as by mean of computer simulations. We analyse the impact of channel non-linearities and group delay distortion, togheter with the benefits of countermeasures at either the transmitter or receiver side, such as dynamic pred-istortion and post-compensation.

Chapter 2

Single Carrier per Transponder

In this chapter we analyse the impact of typical satellite channel impairments on the overall end to end link performance, assuming a Single Carrier per Transponder configuration.

For a specific system architecture, and a selected Modulation and Coding Scheme, performance requirements are specified as the E_s/N_0 ratio needed at the receiver side, for QEF operation over AWGN channel, as introduced in Section 1.1. However, channel impairments shall be taken into account for calculating link budgets, since they worsen the robustness of the transmission chain against noise.

As we will show in the following sections, such impairments can be conveniently considered as additional terms to the overall noise level. As a consequence, the impact of channel impairments can be effectively analysed and quantified via computer simulations of reduced complexity, which do not resort directly to BER calculations, and hence are not based on a specific transmission chain. Figure A.1 shows the reference Simulink Block Diagram which will be used throughout this chapter, for characterising the impact of both group delay variations and non-linear distortion on the transmitted waveform.

2.1 Group Delay Distortion

The satellite channel frequency response is dominated by the IMUX and OMUX filters on board the payload. Typically, these split the total input bandwidth in channels (also referred to as *transponders*) of either 36, 54, 72 or 108MHz. Each channel is frequency converted and amplified separately, before forwarding the signal through the downlink.

This is to combat distortion due to intermodulation products, arising from the power amplifier non-linearity (Section 4.1).

Recall that in practice, the full bandwidth of a digital signal with Symbol Rate R_s, always exceeds the minimum one by a certain factor greater than 1. Since here the focus is always on SRRC transmit and receive filters (Appendix C), the total signal bandwidth is equal to $R_s(1+\rho)$, where ρ is the Roll-Off factor. Hence, in order to avoid filtering out some spectral content, the maximum Symbol Rate shall be less than the channel passband, by an amount depending on the actual excess factor $1+\rho$. In addition, distortion due to the group delay variations in the vicinity of the cut-off frequencies, leads to lower further the maximum Symbol Rate. These considerations applies unless an efficient equalization scheme is applied at either the transmitter or the receiver side, as we shall see in Chapter 3.

2.1.1 A Model for Channel Filters

The IMUX and OMUX filters frequency response are best described in terms of magnitude and group delay variations. Typically, the latter is severe in the pass band boundaries, due to actual technological limitations. This causes a non negligible amount of distortion on the transmitted waveform, when the total signal bandwidth approaches the channel pass band. In [4, H.7] some indications are given on how to model the behaviour of the channel filters. However, here we prefer to focus on some specification masks required by the Satellite Operator. These are given for both magnitude and group delay variations, referring to the *input section* and the *overall section*. The former is dominated by the IMUX filter only, while the latter refers to the frequency response of the transponder as a whole, which is shaped by the cascade of both IMUX and OMUX.

Figure 2.1 shows the baseband model selected for the frequency response of a 36MHz transponder. The IMUX and OMUX have been modelled with IIR digital elliptic filters of order 3, as suggested in [1, Ch. 9]. The effort has been the one of optimizing the filters coefficients in order to skim the mask specifications, so to have a model meant for a worst case scenario.

2.1.2 Estimating The Group Delay Distortion

At the receiver side, due to the non ideal channel frequency response, the SRRC receive filter is not matched to the transmitted waveform spectrum. Hence, after timing and sampling, the received symbols are affected from Inter Symbol Interference with variance σ^2_{ISI}. It turns out that the ISI statistics is well approximated by the complex normal

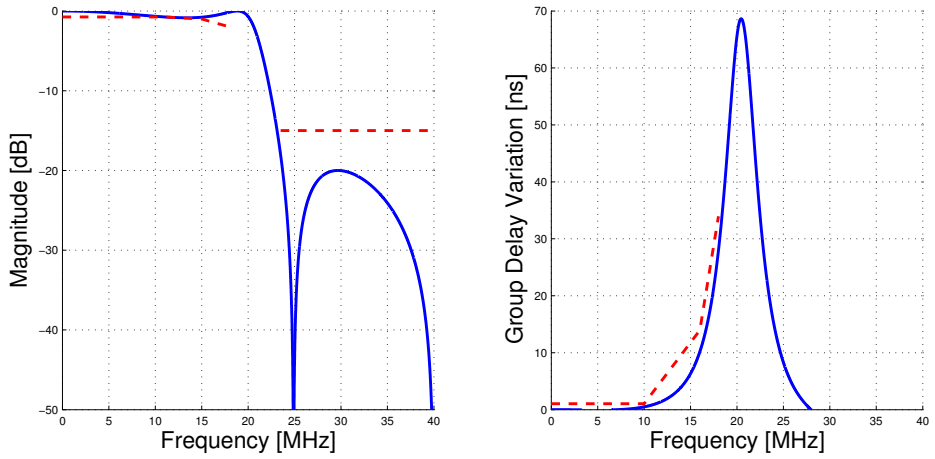

(A) Input Section

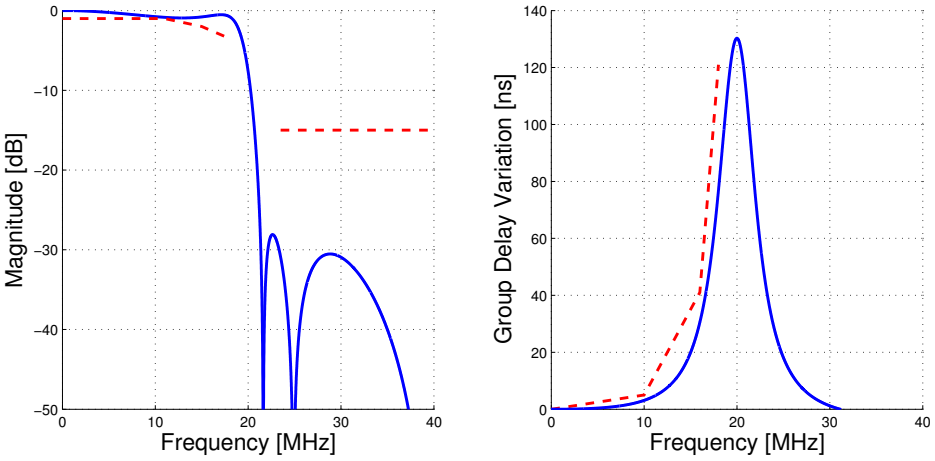

(B) Overall Section

FIGURE 2.1: Channel frequency response model (blu lines) versus specification masks (red dashed lines)

distribution with mean value given by the reference constellation point and the same variance. Hence, the ISI power σ^2_{ISI} can be considered as an additional term to the noise power spectral density at the receiver side. For any System Architecture and a selected Modulation and Coding Scheme, this translates in an higher Es/N_0, required at the decision point for QEF operation. In formulae

$$\left[\frac{E_s}{N_0 + \sigma^2_{ISI}}\right]^{LSC}_{req} [dB] = \left[\frac{E_s}{N_0}\right]^{AWGN}_{req} [dB]. \tag{2.1}$$

Where the superscript LSC (Linear Satellite Channel) refers to the idealised scenario where the dominant channel impairment is indeed the distortion due to group delay variations. Assuming a fixed average symbol energy, this means that the robustness of the system against noise is reduced compared to the ideal AWGN channel.

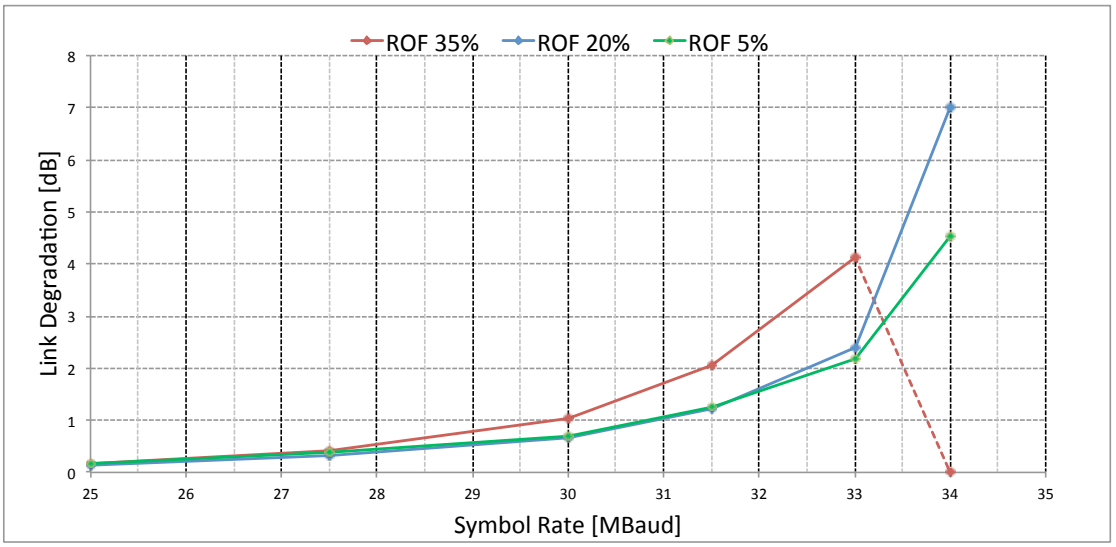

FIGURE 2.2: Link Degradation through a 36MHz transponder, 16APSK 2/3

From 2.1, with basic algebraic operations, we get to

$$\left[\frac{E_s}{N_0}\right]_{req}^{LSC}[dB] = \left[\frac{E_s}{N_0}\right]_{req}^{AWGN}[dB] + \left[1 + \frac{\sigma_{ISI}^2}{N_0}\right]^{LSC}[dB]. \tag{2.2}$$

The quantity $D = 1 + \sigma_{ISI}^2/N_0$ is greater than or equal to one, and estimates of how much the signal to noise ratio shall exceed the reference value over AWGN, in order to meet the same error performance. We remark that Equation 2.2 gives a measure for the Link Performance Degradation over LSC, where the dominant impairment is the distortion due to group delay variations, and depends on the actual Symbol Rate and Roll-Off factor. Furthermore, In the case of fixed average symbol energy, from 2.1 and 2.2 it is straightforward that $\sigma_{ISI}^2 \to N_0^{AWGN} \Rightarrow N_0^{LSC} \to 0^+$, hence *the link becomes intolerant to noise*, and the degradation explodes to $+\infty$.

Figure 2.2 shows the degradation in dB measured in simulation for the channel model of Figure 2.1, for different Symbol Rates and ROFs. We observe the following:

1. For Symbol Rates close to 28MBaud, all ROFs yield roughly the same performance. However, ROF 20% behaves slightly better than the 35% one, which already suffers from band cut-off, and than 5%, which is highly sensible to ISI.

2. As expected, ROF 35% is impractical for Symbol Rates higher than 30MBaud, as degradation explodes due to filters cut-off effect.

3. ROF reduction down to 5% is only beneficial for Symbol Rates beyond 33MBaud, where the degradation reaches levels which may be unacceptable.

Based on these considerations, and if not otherwise specified, in the following we choose to apply ROF 20% for characterizing non-linear distortion, as well as for giving complete results on the total degradation due to the satellite transponder, in single carrier configuration.

2.2 Non-Linear Distortion

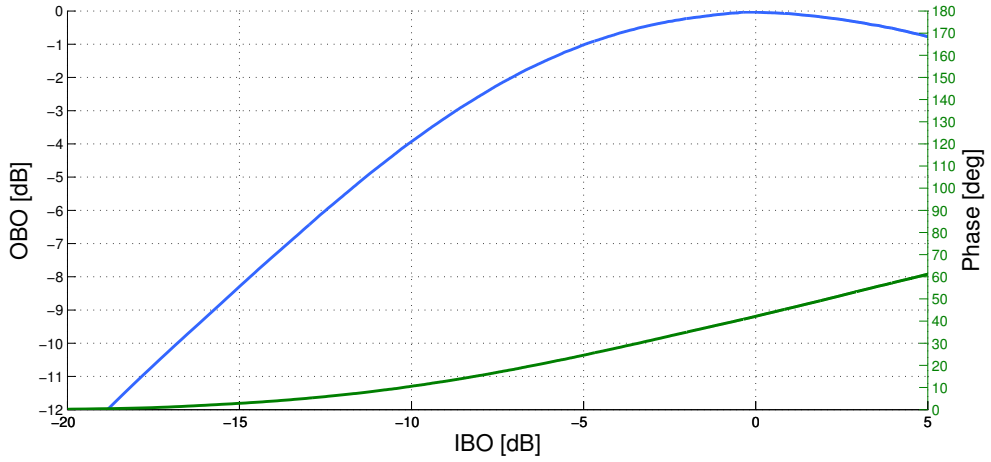

FIGURE 2.3: TWTA Non Linearized Profile, AM/AM and AM/PM curves.

In a satellite transmission chain, the sources of non-linearities are multiple. Among these, the most relevant are the High Power Amplifier at both the ground station and on board the payload. However, the first is typically operated with a large OBO, so to limit the distortion introduced in the uplink. This is feasible because, at the ground station, the HPA dimensions and power supply are not critical. It applies the contrary to the one on-board the satellite, where the total available power is a scarce resource. In the following, we will consider the HPA in orbit as the dominant source of non-linearity on the satellite chain, as suggested in [4].

Figure 2.3 shows the TWTA (Non Linearised profile) introduced in [4]. This latter is often used to model the HPA behaviour as a memoryless non-linearity, assumed as worst case scenario. Its input-output transfer characteristic is best described by mean of the AM/AM and AM/PM curves. In particular, both curves only depend on the amplitude (i.e. power) of the input signal. Figure 2.4 shows the effect of non-linearity on the constellations defined in [4]. The IBO levels chosen for these and the following plots, come from a set of selected *optimum back off levels*, dependent on any given modulation and coding scheme, as we shall see later.

For the moment, we notice the following:

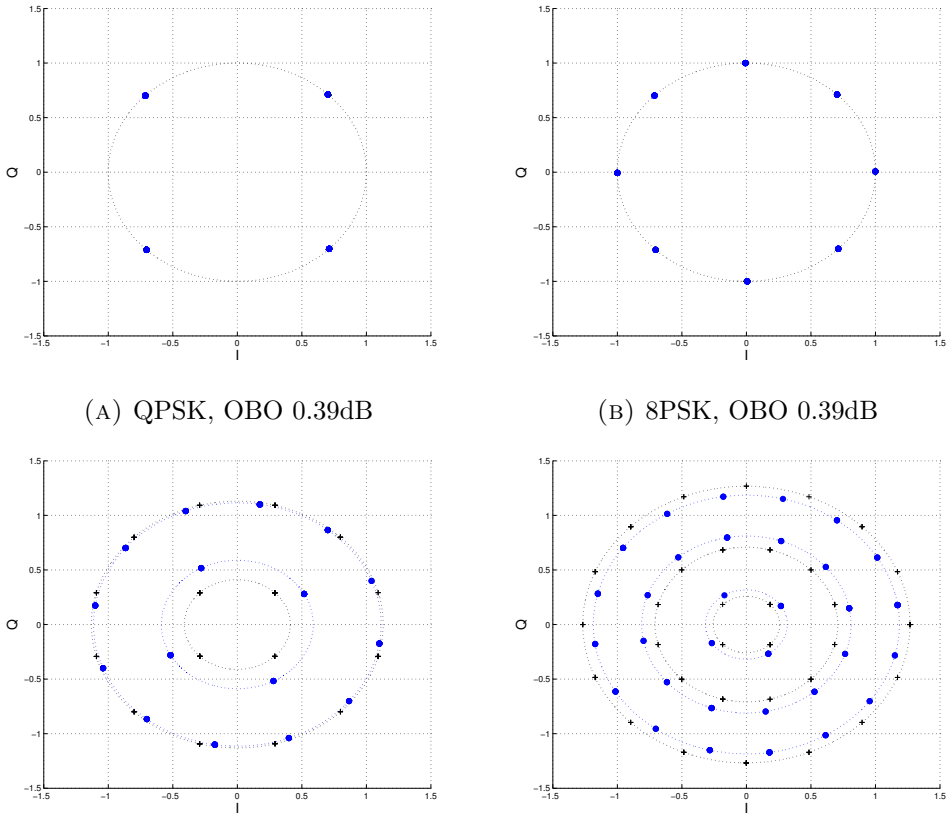

(A) QPSK, OBO 0.39dB

(B) 8PSK, OBO 0.39dB

(C) 16APSK, OBO 1.68dB

(D) 32APSK, OBO 3.77dB

FIGURE 2.4: Constellation warping due to memoryless non-linearity. Reference constellations (black crosses) versur warped constellation points (blue dots)

- for a given reference constellation, the ratios between the radii of different rings are modified,
- all symbols in the reference constellation undergo a phase shift which depends on the ring to which they belong.

These observations translate in the conclusion that the impact of the non-linearity on PSK constellations reduces to a static phase shift, since all symbols belong to a single ring. This can be easily compensated by a phase recovery algorithm at the receiver side. Here we apply the Pilot Aided one suggested in [5]. On the other hand, despite the higher back off level applied, APSK constellations undergo an important warping, and after phase recovery, the relative position between different symbols is altered.

In practice, any symbols constellation is aimed at modulating a selected baseband transmit pulse shape. Figures 2.6a to 2.6c give an idea of the impact of the non-linearity on the modulated baseband waveforms (magnitudes). In the distortion free channel (blue lines), the received waveform is shaped by the convolution of the SRRC transmit and receive filters, hence the overall isolated pulse is of the Raised Cosine type, which is of

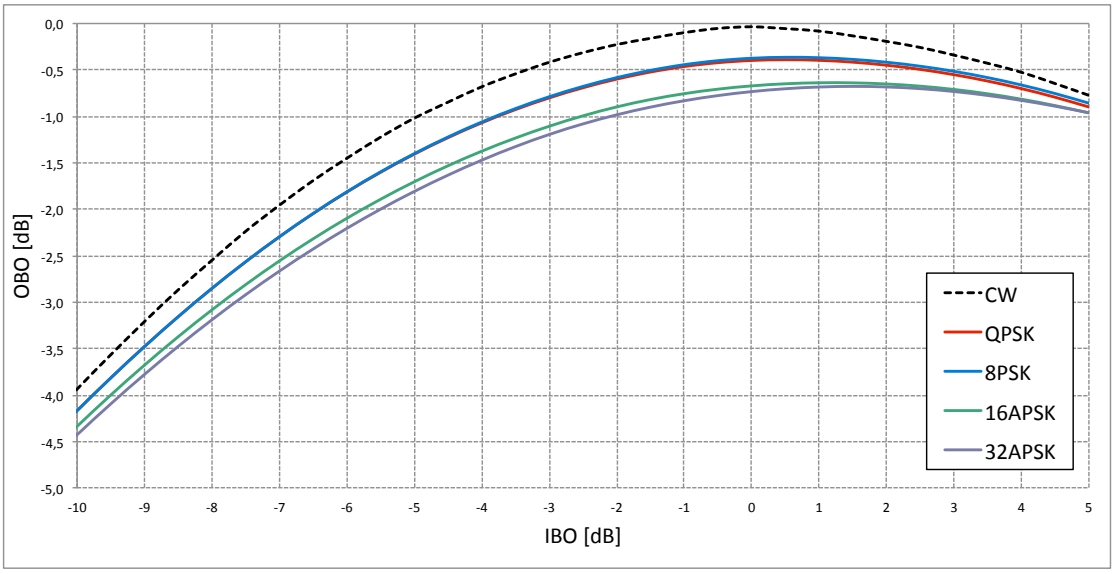

FIGURE 2.5: TWTA Non Linearised Profile AM/AM Characteristics for Modulated Carriers

Nyquist (Appendix C). Assuming perfect timing, this implies that after sampling, the received symbols (blue crosses) are free from ISI. On the other hand, over a non-linear channel, the shape of the transmitted waveform is distorted by the channel non-linearity, hence the SRRC filtered received waveform (red lines) looses the Nyquist property. As a consequence, the received sampled symbols (red crosses) are affected from ISI, and their position is randomly distributed around the warped constellation points.

Figure 2.5, shows the AM/AM characteristic of the TWTA (Non Linearised Profile) for modulated carriers. Applying the non-linearity to a *Continuous Wave* (CW, dotted line), yields exactly the curve of Figure 2.3. However, when the non-linearity is applied to a modulated carrier, in the vicinity of the saturation point, the actual OBO differs from the reference one of approximately -0.4dB for PSK constellations, and -0.7dB for APSK constellations. This is due to the fact that the transmitted BB waveform amplitude, may instantaneously exceed the saturation, thus incurring in clipping. We stress that this result is not dependent on the carrier frequency, nor on the actual symbol rate, but only on the transmitted waveform magnitude, and on the AM/AM transfer characteristic of the TWTA.

In conclusion, due to the channel non-linearity, any symbol constellation undergoes a warping of the reference points in the complex plane, together with the addition of ISI, as sketched in Figure 2.7. Both effects need to be quantified, in order to determine the optimum back-off level for each modulation and coding scheme. The latter is the best trade off between

1. distortion of the constellation due to vicinity at the saturation point,

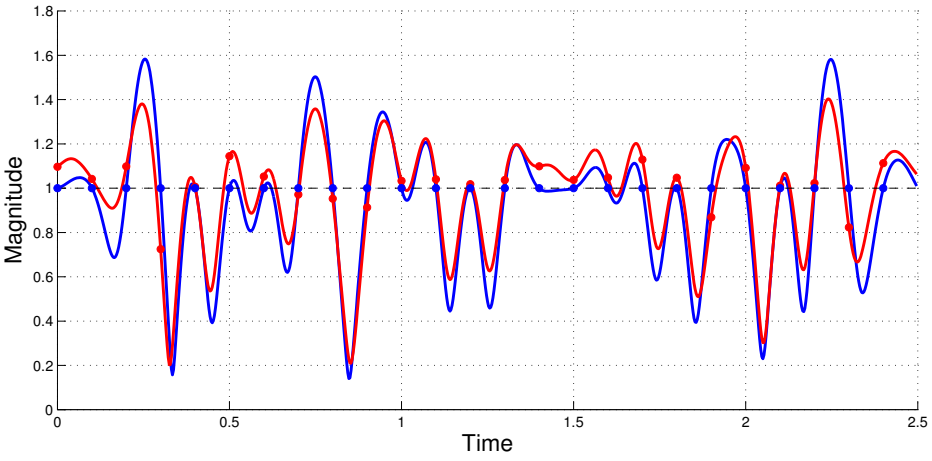

(A) 8PSK, OBO 0.39dB

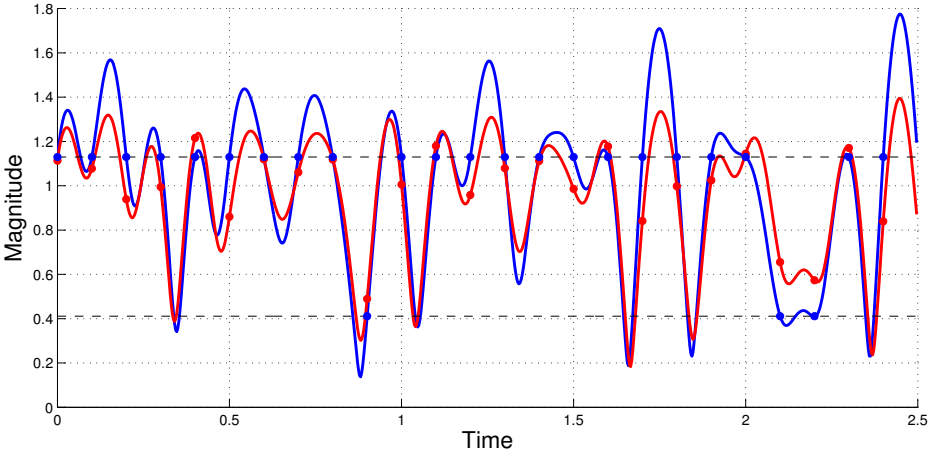

(B) 16APSK, OBO 1.68dB

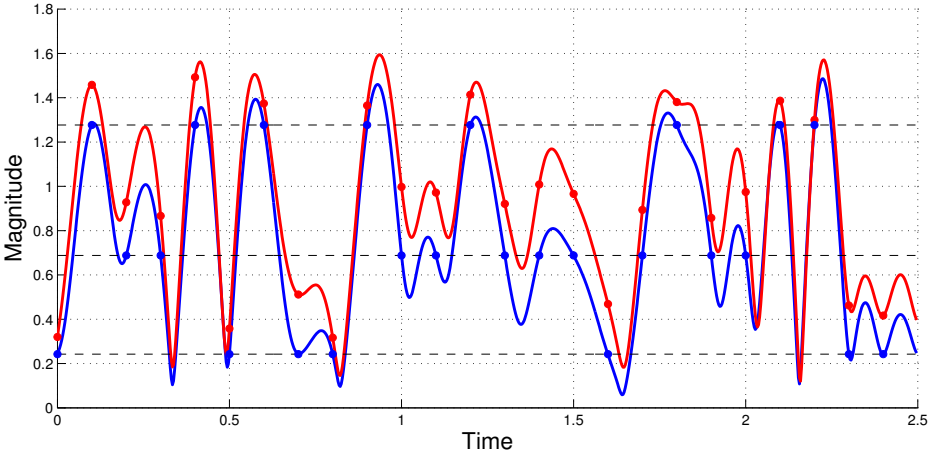

(C) 32APSK, OBO 3.77dB

FIGURE 2.6: Non-linear distortion of BB Modulated Waveform (magnitude). Plots normalized for unit power. Distortion free (blue lines and dots) versus non-linear channel (red lines and dots)

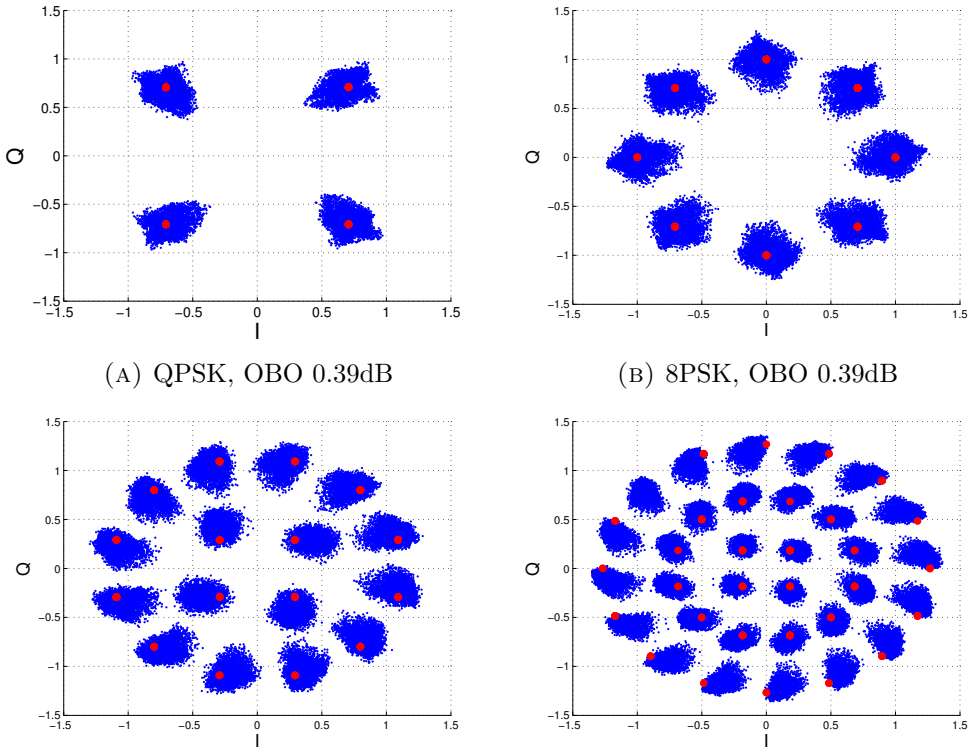

(A) QPSK, OBO 0.39dB

(B) 8PSK, OBO 0.39dB

(C) 16APSK, OBO 1.68dB

(D) 32APSK, OBO 3.77dB

FIGURE 2.7: Impact of the non linearity on the symbol constellations at the decision point, after Phase Recovery. Scatter plots normalized for $E_s = 1$

2. loss in power due to high back-off level,

and minimizes the total *link performance degradation*, as we will argument in detail in the next session.

2.2.1 A measure for non-linear distortion

Channel non-linearities as well reduce the robustness of the end-to-end link against noise. In this context not only the ISI, but also the constellation warping and loss in power due to the back-off applied shall be taken into account. The link performance degradation due to the TWTA non-linearity, can be expressed as

$$D_{tot}[dB] = \left[\frac{E_s}{N_0}\right]_{req}^{NLC}[dB] - \left[\frac{E_s}{N_0}\right]_{req}^{AWGN}[dB] + OBO_{modcarrier}[dB], \tag{2.3}$$

Equation 2.3 is a convex function of the actual Input Back-Off (IBO) level applied to the TWTA, and always has a global minimum, called the *optimum back-off*. This represents the best trade off between the distortion of the transmitted waveform, which increases in

the vicinity of the saturation point, and the loss in power at the output of the TWTA due to the back-off applied, and minimizes the link performance degradation over non-linear channel.

In past works [6], Equation 2.3 had been quantified via computer simulations, applying the channel non-linearity with a certain TWTA profile, to a complete transmission chain, and evaluating the error rate at the receiver side. In this way, D_{tot} represents the delta in dB between the E_s/N_0 required at the decision point for QEF operation over non-linear channel, and the reference (lower) one, required over AWGN. Altough this approach is indeed correct, it requires very computational and time demanding simulations. In addition, using this methodology, it seems that the link degradation is system dependent, when it's not the case. we will now outline an alternative method to quantify 2.3, which relies on the received symbol constellation only, together with the knowledge of the performance in terms of E_s/N_0 for QEF, over AWGN.

According to Figure 2.3, the TWTA introduces a global phase shift on all the symbols centroids in the constellation, which depends on the average symbol energy at the TWTA input. We stress that this static effect can be easily compensated at the receiver side, appliyng a proper phase recovery algorithm.

However, as we already outlined in section 2.2, at the demodulator side, after phase recovery and AGC, the relative positions between different symbols centroids in APSK constellations are altered both in amplitude and in phase. This is because each ring of symbols lies at a different energy level, and hence it is subject to a different transformation through the TWTA.

To fix the ideas, Figure 2.8a depicts the quantities on interest in the analysis of non-linear distortion, with focus on two symbols at different energetic levels in a 16APSK constellation (first quadrant). Note that the received symbols centroids (red dots) are displaced from their reference positions (black dots). With focus on the DVB-S2 specifications [4], this reduces the strength of the system against noise, since the LDPC decoder relies on the log-likelihood informations at the output of the soft demodulator, which are based on the reference non-warped constellation, as well as on the relative position between symbols. Here we propose a measure for quantifying such degradation, which is based on the relative position between symbols having the same phase, but lying on different rings, on the reference constellation.

With reference to Figure 2.8a, let d_{ref} be the distance between the two symbols having phase $\pi/4$ and lying on the two different rings of a 16APSK constellation (first quadrant), and d_{warp} its warped version. Then $err^2 = (d_{ref} - d_{warp})^2$ is defined as the energy

of the distance difference between corresponding points in the reference and warped constellations, and depends on the displacement of both symbols.

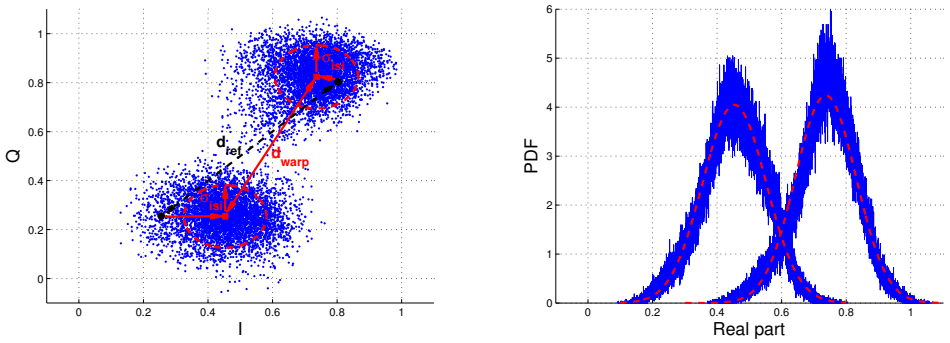

(A) Pictorial View (B) ISI Histograms

FIGURE 2.8: Illustration of quantities involved in distortion estimation for 16APSK.

Two observations follow:

1. In PSK constellations, the distance difference measure is not even defined, because all symbols lie on the same ring. In this case, the pilot based AGC and phase recovery algorithm brings all symbols back in their reference positions on the complex plane, since the pilot itself belongs to the same ring.

2. In APSK constellations with more than 2 rings, the distance difference measure is defined between the innermost and the outermost rings.

To justify Observation 2, and with reference to Figure 2.9b, let's focus on the 32APSK, which has three concentric rings. Notice that the symbols with phase $\pi/4$ on the innermost and middle rings undergo a displacement, but *towards the same direction*. More in general, no symbol in the constellation gets closer to the one belonging to the innermost ring, and hence the related soft informations at the LDPC input will reasonably not be affected. On the other hand, the outermost ring shirks in the opposite direction, and is subject to a sensibly different phase shift. As a conclusion, the relative position between symbols belonging to the innermost and outermost rings is warped affecting negatively the soft demodulation.

In addition, the warped constellation points are affected from ISI, which can be modelled as a complex random variable having mean $a_{rx,m}$, and variance $\sigma^2_{ISI,m}$ for $m = 1 \dots M$. In this case the ISI variance is different for symbols belonging to different rings, nominally *the higher the ring energy level, the higher the ISI variance*. Figure 2.8b plots the histograms of selected received symbols (real part), together with the theoretical gaussian probability density function, having the same mean and variance (red dashed

line). The match is indeed acceptable, and it increases with the constellation order, as we expect from the Central Limit Theorem.

Now, taking a cue from Equation 2.2, we infer the empirical relation

$$\left[\frac{E_s}{N_0}\right]_{req}^{NLC}[dB] = \left[\frac{E_s}{N_0}\right]_{req}^{AWGN}[dB] + \left[1 + \frac{\sigma_{ISI}^2 + err^2}{N_0}\right]^{NLC}[dB]. \tag{2.4}$$

where $\sigma_{ISI}^2 = 1/M \sum_{m=0}^{M-1} \sigma_{ISI,m}^2$ is the average of ISI variance. Then, by replacing 2.4 in 2.3, we get

$$D_{tot}[dB] = \left[1 + \frac{\sigma_{ISI}^2 + err^2}{N_0}\right]^{NLC}[dB] + OBO_{modcarrier}[dB]. \tag{2.5}$$

Equation 2.5 seeks to weight the loss in performance due to constellation warping together with the effect of ISI, in the expression of the total link performance degradation. This is a heuristic approach, whose effectiveness has been be compared with former results achieved at Eutelsat and at the European Space Agency, as we will see shortly.

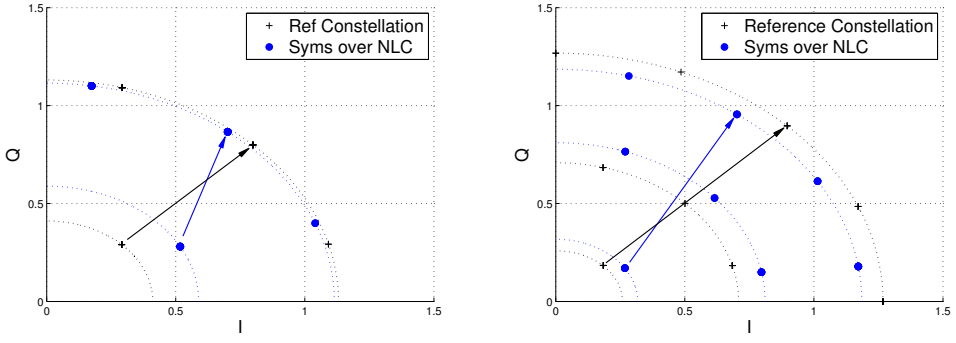

(A) 16APSK (B) 32APSK

FIGURE 2.9: Illustration of symbol displacement for APSK constellations, first quadrant.

2.2.2 The algorithm devised

With reference to the Block Diagram of Figure A.1, and neglecting the impact of the channel filters, the procedure for finding the *optimum back off* consists in the following steps:

1. Choose a particular Modulation and Coding scheme, whose performance is meant for a specific System Architecture. Recall that in this work we focus on the DVB-S2 specifications [4], if not otherwise specified.

2. Choose the Roll-Off factor ρ for the SRRC pulse shaping and matched receive filters. Here we assume $\rho = 0.20$.

3. Choose a particular TWTA transfer characteristic. Here we consider the Non-linearised profile introduced in [4].

4. Sweep the IBO level among the AM/AM transfer characteristic of the TWTA, with a step of 1dB.

5. For each IBO value, run the block diagram of Figure A.1. We process 10^4 of symbols for each constellation element. Hence roughly $M \times 10^4$ symbols in total shall be considered, for precision of variance estimates.

6. Estimate the Output Back Off at the TWTA output.

7. Knowing the transmitted integer symbols α_{tx}, sort the corresponding warped and ISI corrupted received complex ones. Then estimate the centroids $a_{rx,m}$, hence err^2 and finally $\sigma^2_{isi,m}$ for $m = 1 \dots M$.

8. compute 2.5.

2.2.3 Simulation Results

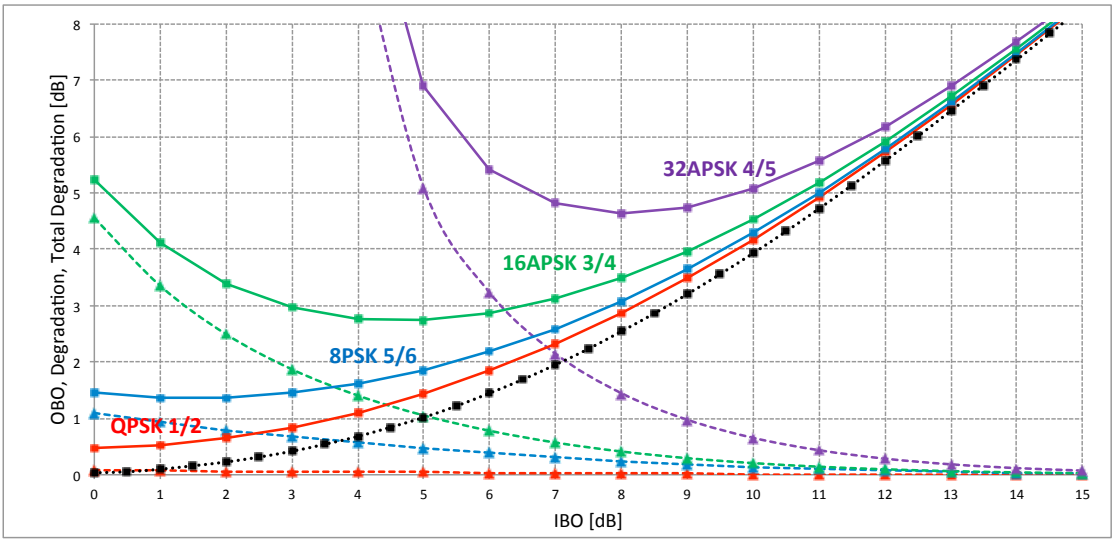

FIGURE 2.10: Link degradation due to channel non-linearity, for different MODCODs in the DVB-S2 specifications. The OBO curve (black dotted line) is referred to an unmodulated Continuous Wave.

Figure 2.10 shows some link degradation curves in the non-linear channel, where the link degradation is dominated by the TWTA Non-linearised profile.

Figure 2.11 compares the performance required to achieve the MODCOD dependent spectral efficiencies of the DVB-S2 specifications, over both AWGN and non-linear channel. The signal to noise ratio here is best expressed in terms of C_{sat}/N i.e. as the ratio between the carrier power available when the TWTA is driven in saturation, versus $N = N_0 \times R_s$, i.e. the noise power on a bandwidth equal to the nominal symbol rate. Notice that the performance of PSK constellations over non-linear channel worsen in a small extent only. This is the main reason why in the last decades they had always been preferred for digital satellite communications, as the TWTA can be driven very close to saturation, exploiting all the available power in the downlink. On the other hand, APSK constellations, although optimized to achieve better performance over non-linear channel than classical QAM, is subject to an important degradation, which increases considerably their working point, according to 2.5.

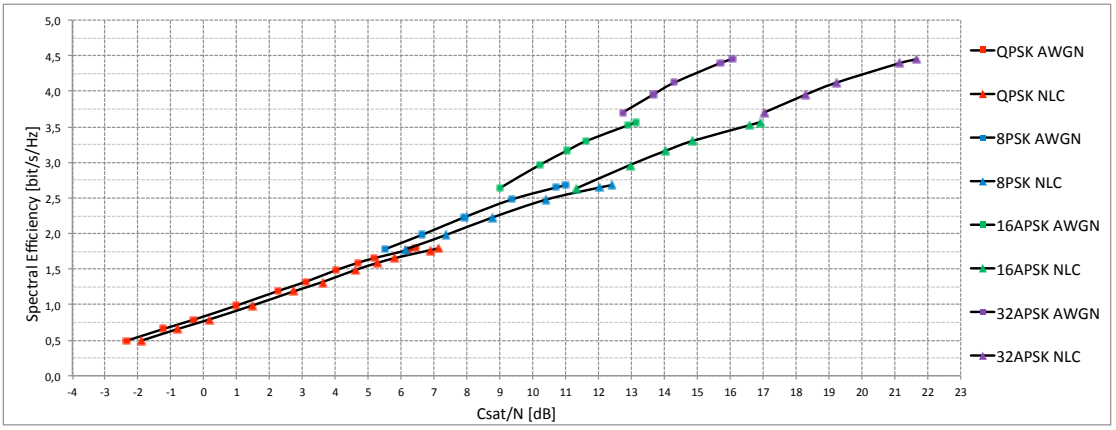

FIGURE 2.11: Spectral efficiency versus required C_{sat}/N for DVB-S2 specifications.

2.3 Total Link Degradation

The results on link degradation devised in sections 2.1 and 2.2 apply for ideal channels where group delay variations and non-linear distortion are considered separately. However, in all the practical satellite transmission chains, such impairments jointly impact the link performance. Note that we can't draw correct conclusions about the *total link degradation* by addition of the two contributions, as the cascade made by the IMUX - TWTA - OMUX is a mixed linear and non-linear system, and the superposition principle doesn't hold. It can be verified in simulation that the overall degradation approaches the addition of the three contributions when the TWTA operated in the linear region, for high OBO values. however this is not a case of interest for the Satellite Operator, which seeks to operate the TWTA *the closer possible* to the saturation, i.e. at the optimum back-off level, as discussed in Section 2.2. As a conclusion, we run the algorithm of

section 2.2.1 considering this time the full chain of Figure A.1 for selected MODCODs, ROFs and Symbol Rates.

We choose to neglect the power loss due to the channel filters. It accounts for roughly 0.25dB for the IMUX and for 0.15dB for the OMUX. This is because the former can be easily compensated increasing the power in the uplink, the latter can be included in C_{sat} for Link Budget calculations.

MODCOD	**QPSK 1/2**		**QPSK 2/3**		**8PSK 3/5**		**8PSK 5/6**	
ROF / **R_s**	20%	5%	20%	5%	20%	5%	20%	5%
27.5Mbaud	0.54	-	0.58	-	0.85	-	1.62	-
30.0Mbaud	0.59	-	0.72	-	1.00	-	2.08	-
32.5Mbaud	0.81	0.87	1.09	1.19	1.71	1.91	4.80	5.63
36.0Mbaud	1.82	1.79	3.02	2.95	7.28	6.98	*NA*	*NA*

TABLE 2.1: Total degradation in dB for PSK MODCODs, over a 36MHz transponder. Values referred to the optimum back-offs of table 2.2.

.

Table 2.1 shows the total transponder degradation for PSK modulated waveforms, where we apply the model of Figure 2.1 and the TWTA profile of Figure 2.3. We observe the following:

1. QPSK modulated carriers can exploit the whole transponder pass band. In fact, with focus on the last row of the table, we notice that even when the Symbol Rate alone approaches the channel bandwidth, the distortion due to group delay variation and cut-off effect of the filters accounts for 1.5dB to 2.5dB of extra degradation. This is acceptable, since the QPSK MODCODs defined in [4] have very low performance requirements over AWGN (Table 2.2).

2. In order to keep the transponder degradation at acceptable levels, 8PSK modulated carriers shall not fill the transponder bandwidth by more than 30-32.5Mbaud, depending on the *coding strength*.

3. Applying a Roll-Off reduction down to 5% is not beneficial. This yields a very small gain when the symbol rate approaches the transponder pass band, and is self-defeating otherwise.

Note that, an effective equalization scheme at either the transmitter or the receiver side, may minimize the group delay distortion [7], thus improving link performance when the total signal bandwidth does not exceeds considerably the transponder pass band.

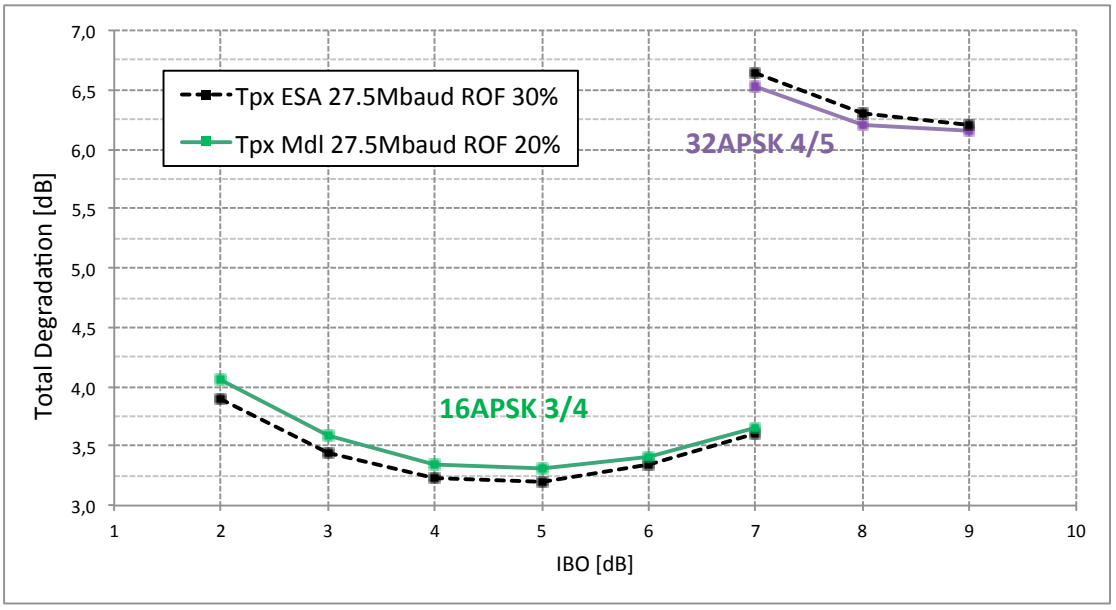

FIGURE 2.12: Total degradation curves for APSK constellations, compared with results published by ESA.

Figure 2.12 shows the total link degradation curves for both the 16APSK 3/4 and 32APSK 4/5, for the transponder model devised. In addition, a comparison is made with some reference points published by Gaudenzi *et al* in [6], which are meant for a 30% ROF, and a less critical channel frequency response. In particular, the latter was assumed as maximally flat in the passband for both the IMUX and OMUX filters, while the group delay variation is non negligible only starting from a 12MHz deviation from the centre frequency.

Note that, despite the transponder model and the Roll-Off are different, the curves in Figure 2.12 match with a good approximation, and yield the same optimum back-offs.

In conclusion, Table 2.2 shows the selected optimum back-off and relative total link degradation for all the MODCODs included in the DVB-S2 specifications, for the 36MHz transpinder presented in this chapter, and assuming ROF 20%, $R_s = 27.5$Mbaud, TWTA Non Linearised Profile.

MODCOD	Spectral Efficiency [bit/s/Hz]	Ideal E_s/N_0 [dB]	IBO [dB]	OBO [dB]	D_{tot} [dB]
QPSK 1/4	0.490243	-2.35	0.0	0.39	0.46
QPSK 1/3	0.656448	-1.24	0.0	0.39	0.48
QPSK 2/5	0,789412	-0.30	0.0	0.39	0.50
QPSK 1/2	0.988858	1.00	0.0	0.39	0.54
QPSK 3/5	1.188304	2.23	0.0	0.39	0.59
QPSK 2/3	1.322253	3.10	0.0	0.39	0.63
QPSK 3/4	1.487473	4.03	0.0	0.39	0.69
QPSK 4/5	1.587196	4.68	0.0	0.39	0.74
QPSK 5/6	1.654663	5.18	0.0	0.39	0.78
QPSK 8/9	1.766451	6.20	0.0	0.39	0.89
QPSK 9/10	1.788612	6.42	0.0	0.39	0.92
8PSK 3/5	1.779991	5.50	0.0	0.36	0.84
8PSK 2/3	1.980636	6.62	0.5	0.39	0.98
8PSK 3/4	2.228124	7.91	0.5	0.39	1.21
8PSK 5/6	2.478562	9.35	1.0	0.43	1.56
8PSK 8/9	2.646012	10.69	1.0	0.43	2.06
8PSK 9/10	2.679207	10.98	1.0	0.43	2.20
16APSK 2/3	2.637201	8.97	4.0	1.39	2.74
16APSK 3/4	2.966728	10.21	5.0	1.69	3.31
16APSK 4/5	3.165623	11.03	5.0	1.68	3.75
16APSK 5/6	3.300184	11.61	6.0	2.07	4.06
16APSK 8/9	3.523143	12.89	7.0	2.52	4.92
16APSK 9/10	3.567342	13.13	7.0	2.52	5.11
32APSK 3/4	3.703295	12.73	8.0	3.20	5.42
32APSK 4/5	3.951571	13.64	9.0	3.77	6.15
32APSK 5/6	4.119540	14.28	9.0	3.76	6.69
32APSK 8/9	4.397854	15.69	10.0	4.40	8.27
32APSK 9/10	4.453027	16.05	11.0	5.10	8.77

TABLE 2.2: E_s/N_0 performance at QEF for DVB-S2 specifications, optimum back off and total link degradation for 36MHz transponder (TWTA Non Linearised profile, ROF 20%, R_s = 27.5Mbaud)

Chapter 3

Improving Link Performance

The link degradation experienced by APSK modulated waveforms makes counterproductive driving the HPAs of the transmission chain close to saturation. As a consequence, it is not possible to fully exploit all the available power in downlink. Considering also the relatively high SNRs required by the the MODCODs based on multilevel constellations (see Table 2.2), it turns out that the spectral efficiencies yielded by the latter, are just not reachable in practice for brodcasting systems, and only viable for professional application with an inefficient use of ACM. In this chapter we analyse three possible countermeasures to minimize the impact of satellite channel impairments on the overall link performance. Such techniques enable improving the transponder utilisation, since they allow safely reducing the optimum-back off for APSK constellations, and increasing the signal bandwidth at the same time.

3.1 Pre Compensation Techniques

3.1.1 Static Pre-distortion

Recall from section 2.2.1 that the constellation warping effect constitutes an important component in the evaluation of 2.5. This is because the log-likelihood informations, calculated by the soft demodulator at the receiver side, rely on the reference unwrapped constellation. However, the displacement of the received symbols centroids is a deterministic function of the TWTA profile, and of the actual IBO applied. Hence, it can be compensated at either the receiver or the transmitter side.

In the first case, the post compensation involves optimizing the soft demodulation, which should rely on the warped constellation, rather than on the reference one. However, this turns in an added complexity at the receiver side, which may be impractical for consumer

applications [6]. A second solution consists in modifying the signal waveform at the transmitter side. This allows pre-compensating the effect of the TWTA non-linearity, so that at the receiver side all symbol centroids are *brought back* to their reference position.

In [6] an LMS based adaptive algorithm is devised, which computes iteratively the pre-distorted transmit constellation. This is done offline in simulation, in the absence of AWGN, and for a specific TWTA profile and IBO. Each loop iteration consists of three steps:

1. Apply a random seed to the simulation block diagram
2. Generate a window of W symbols at the SRRC receive filter sampler output
3. Compute the error signal at the end of each block
4. Update the pre-distorted constellation.

The last two tasks are achieved using the following equations:

$$\rho_c^{(n)}(s)exp\{j\theta_c^{(n)}(s)\} = \frac{1}{W} \sum_{k\in l^{(n)},\ sW+1\leq k\leq (s+1)W} r(k), \quad n = 1,\ldots,M, s = 1,\ldots,S. \tag{3.1}$$

$$|e^{(n)}(s)| = \rho_c^{(n)}(s) - \rho_{ref}^{(n)} \tag{3.2}$$

$$\rho_{tx}^{(n)}(s+1) = \rho_{tx}^{(n)}(s) - \gamma|e^{(n)}(s)|. \tag{3.3}$$

$$\psi(s) = \begin{cases} arg\{e^{(n)}(s)\} - 2\pi & \text{if } arg\{e^{(n)}(s)\} > 2\pi \\ arg\{e^{(n)}(s)\} + 2\pi & \text{if } arg\{e^{(n)}(s)\} < 2\pi \\ arg\{e^{(n)}(s)\} & \text{otherwise} \end{cases} \tag{3.4}$$

$$\theta_{tx}^{(n)}(s+1) = \theta_{tx}^{(n)}(s) - \gamma\psi(s) \tag{3.5}$$

where S is the total number of iterations, subscript indices c and tx refer to the actual received symbols centroids and transmit constellation respectively, γ is the algorithm adaptation parameter, and $\rho_{tx}^{(n)}exp\{j\theta_{tx}^{(n)}\}$, $n = 1,\ldots,M$ is the pre-distorted constellation at the end of the algorithm execution. In operation, the pre-distorted constellation is loaded into a look-up table which is addressed in real time by the modulator, depending on the actual transmitted symbol.

We found that by choosing $\gamma = 0.1$ and $W = 10^4$, all received symbols centroids are *brought back* at their reference position after $S = 75$ iterations. Figure 3.1 depicts the results for both the 16APSK and 32APSK. The static pre-distortion restores the original ratios between different radii amplitudes, and compensates the global constellation phase shift as well as the relative ones (sec 2.2). Note that, if the DAGC and Phase Recovery

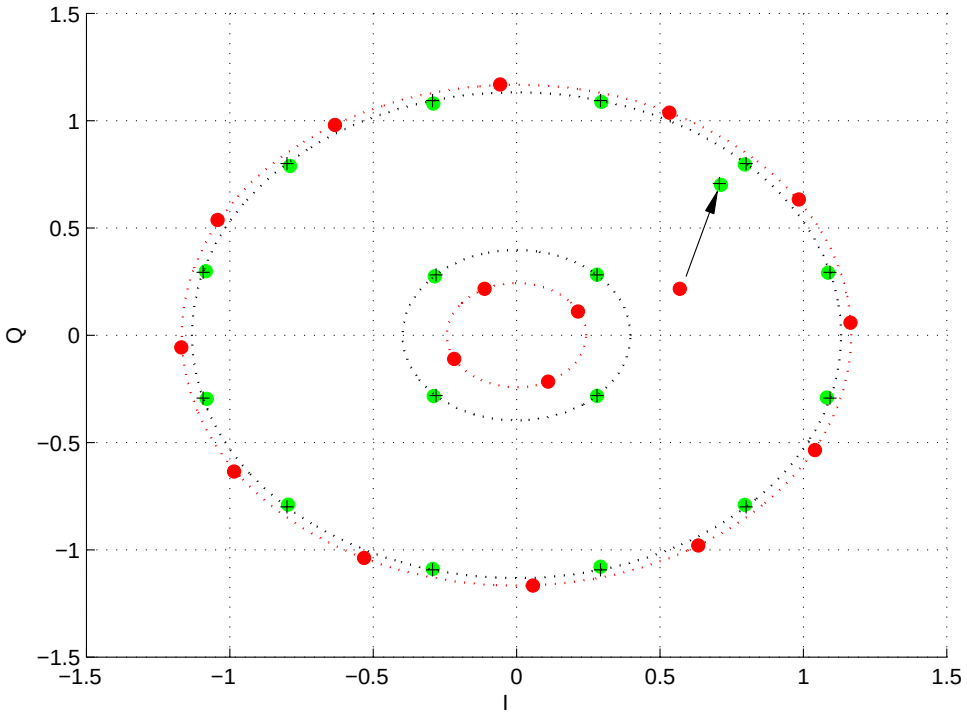

(A) 16APSK

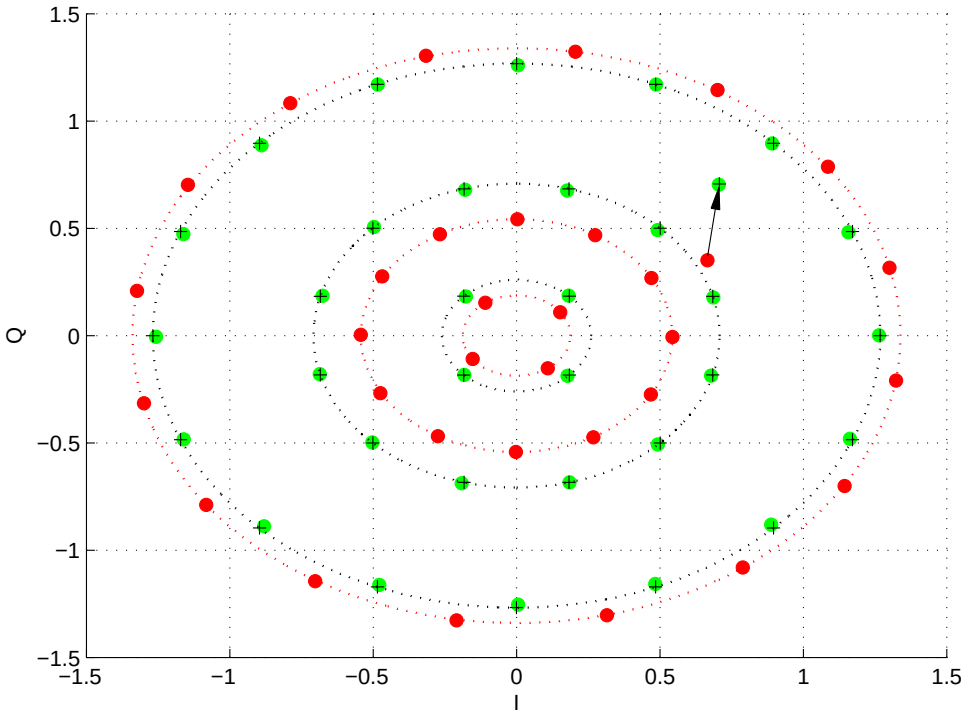

(B) 32APSK

FIGURE 3.1: Static pre-distortion on APSK constellations. Pre-distorted constellation (red dots) versus received symbols centroids (green dots).

algorithms rely on the pilot symbols, as it is the case here, the static pre-distortion shall be applied to the pilot symbol as well, as shown in Figure 3.1. For completeness, we stress that for the simulation sake, and unlike any real case, the TWTA is considered as the only source of phase shift on the constellation, and therefore the phase recovery algorithm becomes unnecessary.

3.1.2 Dynamic Pre-distortion

Despite the static pre-distortion restores the symbols centroids, it doesn't reduce the Inter Symbol Interference at the decision point. In Chapter 2 we approximated the ISI as a Gaussian Distributed random variable, with reference to its statistical second order description σ^2_{isi}. This proved a successful assumption to quantify the impact of channel impairments on the robustness of the System against noise.

However, the nature of ISI *is not random*, and depends mostly on the Transponder characteristics, which here we summarize with the channel filters and the TWTA non-linearity. The dynamic pre-distortion algorithm devised in [6] allows reducing the clustering effect around the constellation centroids, by exploiting the memory of the channel. This means that the pre-distorted constellation is not conditioned only on the current transmitted symbols, as in Equation 3.1, but also on the $(L-1)/2$ preceding and $(L-1)/2$ following symbols (L symbols in total). This calls for an increased look-up table size of $T = M^L$ symbols.

The dynamic pre-compensation is in turn performed offline on a target constellation, based on the channel frequency response (dominated by the IMUX and OMUX filters), the TWTA Profile and the IBO applied. The modulator will then read in real time the look-up table, with an address determined by the current and the $(L-1)/2$ pre-cursors and post-cursors transmitted symbols. With focus on the algorithm implementation, there are two main significant differences respect the steps to be performed for static pre-distortion. First, the simulation block diagram shall now involve the whole transponder model, rather the TWTA non-linearity only. In addition, the look-up table aimed to pre-compensating the transmit constellation, at the modulator side, is now an L-Dimensional one.

In practice, to meet specific real time constraints, L shall not be grater than 5, that is 2 pre-cursors and post-cursors are taken into account. However, it is also straightforward to think that increasing the memory wouldn't produce significant improvements on ISI reduction, at least not to justify the consequent complexity. Actually, for $M = 32$, and considering the pilot symbol, the number of entries is already of the order of $33^5 \approx 4{\times}10^7$. It follows that $L = 3$ *is the only feasible memory for constellations of order 32 and higher.*

On the other hand, simulation results show that, although feasible, considering a channel memory of $L = 5$ brings improvements of less than 0.1dB on link performance for PSK constellations. In conclusion here we choose $L = 3$ for all the constellations in [4].

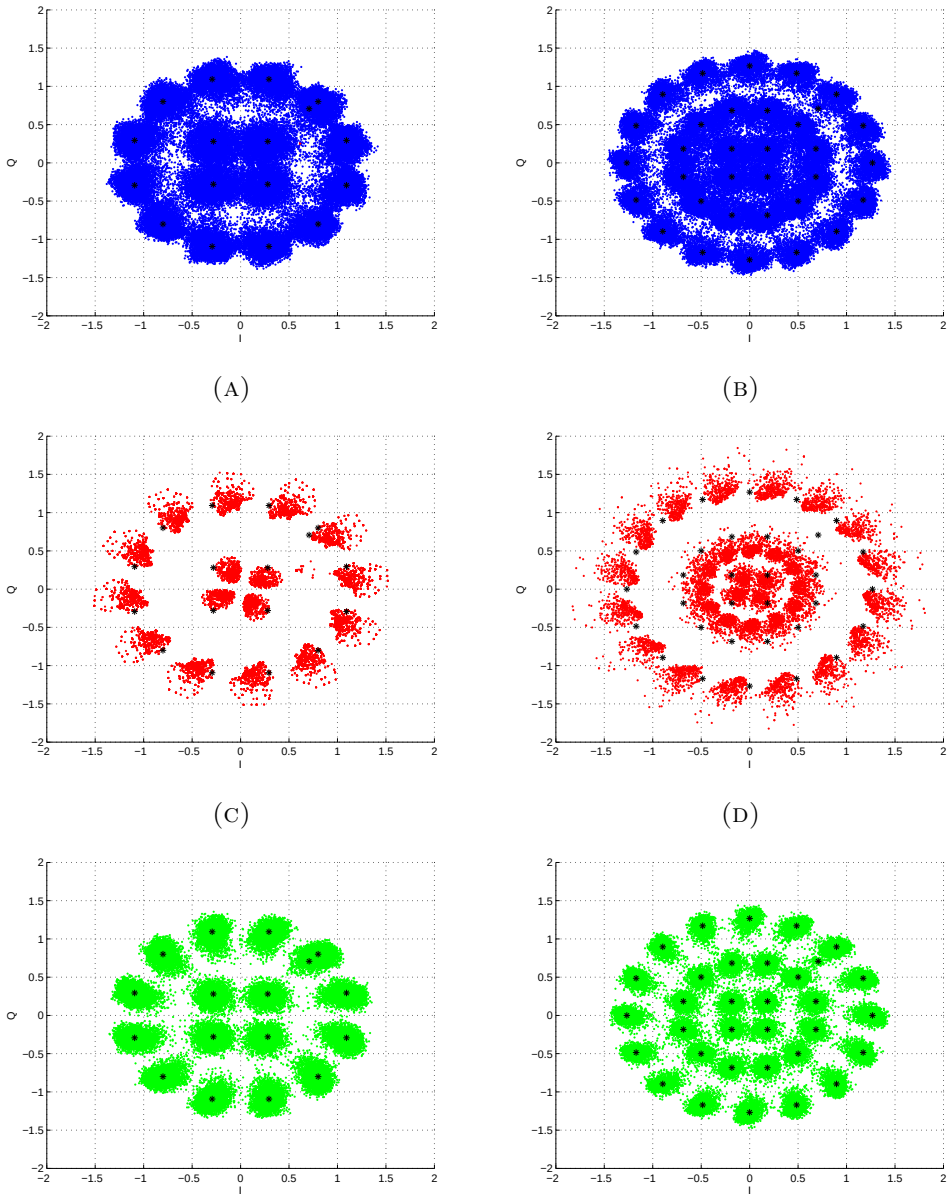

FIGURE 3.2: Dynamic Pre-distortion based on transponder model for 16APSK (IBO 2dB) and 32APSK (IBO 5dB). A-B Received symbols with no pre-compensation, C-D pre-distorted constellations, E-F received symbols with dynamic pre-distorsion.

Figure 3.2 shows qualitatively the improvement of dynamic pre-distortion on the APSK constellations, for a Symbol Rate of 27.5Mbaud. Looking at 3.2c and 3.2d it appears the ISI reduction comes at the expenses of an increased outer constellation points amplitude. In fact, for a fixed IBO and adaptation gain, increasing the number of algorithm iterations reduces the ISI but also increases the OBO. This is because of the increased

Peak to Average Power Ratio and the TWTA clipping effect. As a consequence, the optimum number of iterations is not determined simply by the centroids RMS, but the *cost function* to minimize is of the type of Equation 2.5, where now the dependency is not on the IBO, which is fixed, but on the total number of algorithm iterations S. We found the optimum trade off applying $\gamma = 3 \times 10^{-2}$ and $S = 20, 30, 50, 80$ for QPSK, 8PSK, 16APSK and 32APSK respectively. In all cases the initial constellation was the static pre-distorted rather than the reference one, in order to speed up the algorithm execution.

3.1.3 Simulation Results

We present here our results in simulation, concerning the improvements of pre-compensation techniques. All refer to ROF 20%, as discussed in Chapter 2. We also encourage the reader to compare what follows with the performance declared by Newtec in [8, Table 2.1] and referring to *Equalink*®, the implementation the company offers into its professional modulators.

MODCOD	**QPSK 1/2**		**QPSK 2/3**		**8PSK 3/5**		**8PSK 5/6**	
R_s	TD	Δ	TD	Δ	TD	Δ	TD	Δ
27.5Mbaud	0.52	0.01	0.57	0.01	0.68	0.17	1.04	0.61
30.0Mbaud	0.54	0.05	0.62	0.10	0.74	0.26	1.19	0.89
32.5Mbaud	0.62	0.19	0.74	0.35	1.01	0.70	1.95	2.85
36.0Mbaud	1.00	0.82	1.33	1.69	2.09	5.19	6.13	> 10

TABLE 3.1: Total Degradation in dB for PSK MODCODs with dynamic pre-distortion, and gain versus performance without pre-compensation.

.

Table 3.1 summarizes the performance for selected PSK MODCODs in the DVB-S2 standard, together with the gain in dB on the values of Table 2.1. As known, in this case the optimum back-off is already close to the TWTA saturation, so that it can't be reduced any further. However, consider an increase up to 0.1dB in the OBO values of Table 2.2, according to what discussed in section 3.1.2. On the other hand, there is a net link performance improvements when the Symbol Rate approaches the transponder pass band, which becomes more and more relevant for *higher* MODCODs. In conclusion, the dynamic pre-compensation is able to recover not only the distortion due to channel non-linearity, but *it enables equalizing the channel frequency response at the transmitter side*. In practice, commercially available demodulators often perform equalization by

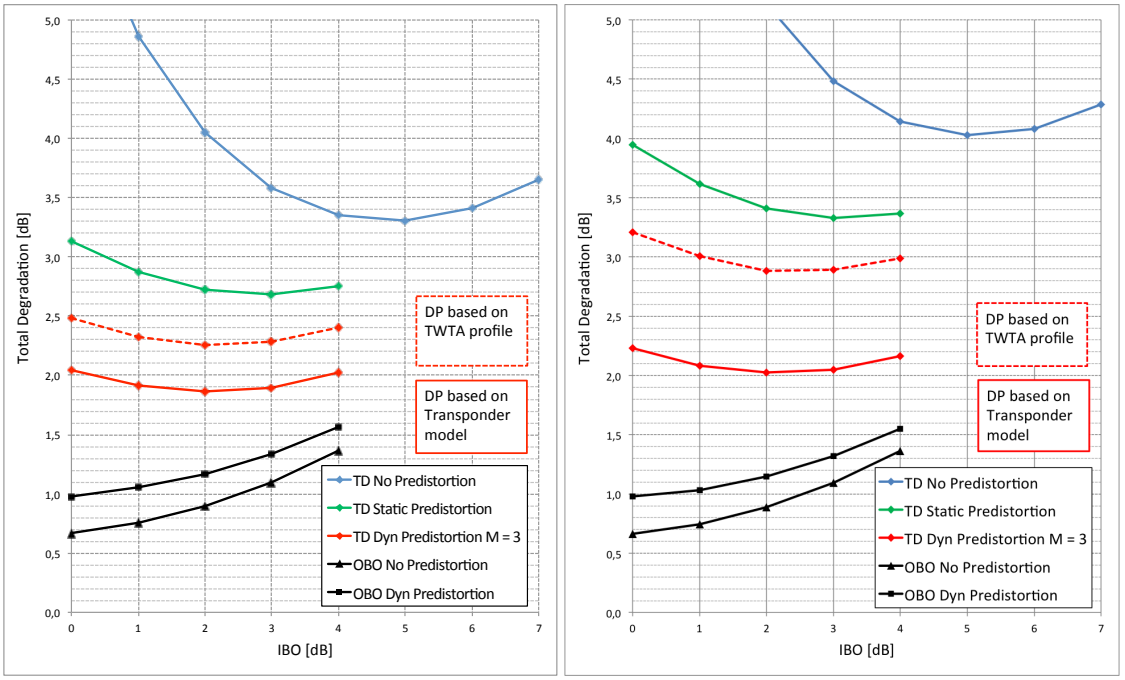

(A) Symbol Rate 27.5Mbaud (B) Symbol Rate 30Mbaud

FIGURE 3.3: 16APSK 3/4 simulated performance. Dynamic Pre-distortion optimized for 45 iterations.

default at the receiver side [7] so that one may expects some further improvement on performance in both pre-distorted and non pre-distorted waveforms.

Figures 3.3 and 3.4 show the performance simulated for 16APSK 3/4 and 32APSK 4/5 respectively. We observe the following:

1. The static pre-distortion alone yields a reduction of the Total Link Degradation of 0.6dB for 16APSK and 1.3dB for 32APSK, compared to the non pre-distorted waveform at the same Symbol Rate. Furthermore, it reduces considerably the optimum back-off in both cases.

2. The dynamic pre-distortion lowers the Total Link Degradation down to 2dB for 16APSK and to 3.1dB for 32APSK, and it is robust against group delay distortion when increasing the Symbol Rate.

3. For a fixed IBO, the pre-distorted waveforms increases the TWTA OBO of roughly 0.2dB for 16APSK and 0.4dB for 32APSK.

The performance concerning dynamically pre-distorted waveforms are achieved when the pre-distortion algorithm is based on an accurate model for the Transponder, and in particular

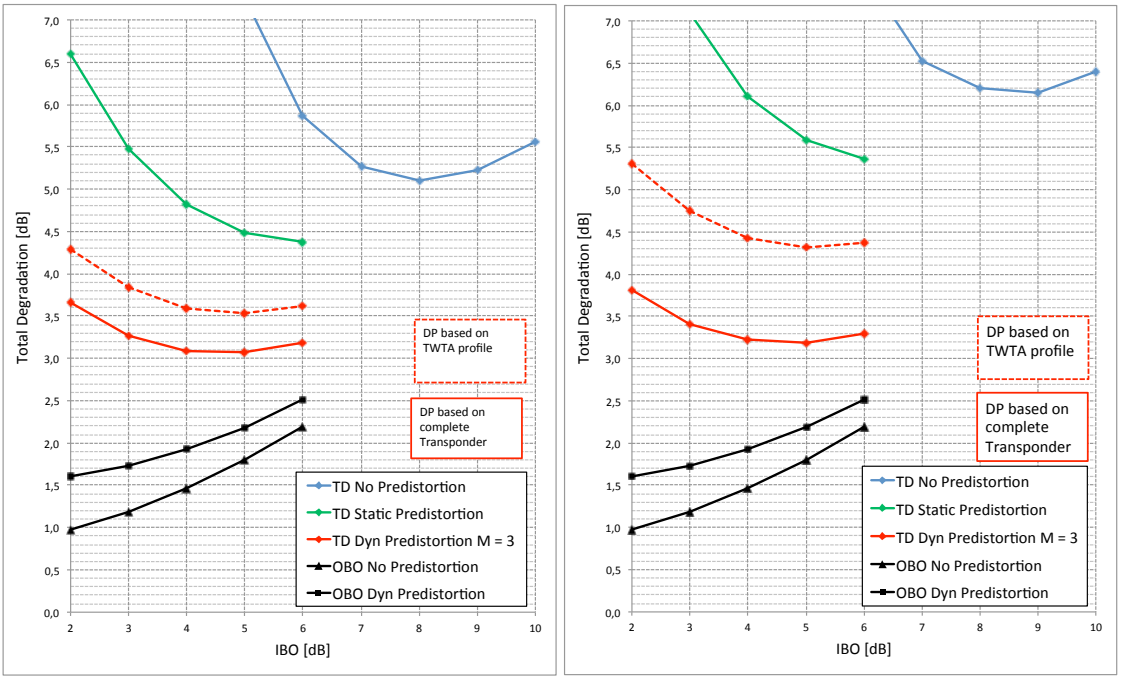

(A) Symbol Rate 25Mbaud (B) Symbol Rate 27.5Mbaud

FIGURE 3.4: 32APSK 4/5 simulated performance. Dynamic Pre-distortion optimized for 75 iterations.

- the channel frequency response (amplitude and group delay variation),
- the actual Symbol Rate,
- the TWTA Profile,
- the actual IBO.

In practice, the channel frequency response is measured with the satellite in orbit, by sweeping in frequency an unmodulated carrier. Hence only the *overall section* frequency response is typically available. In this case, the pre-distortion algorithm runs on a simplified transponder model, where the cascade IMUX - TWTA - OMUX reduces to TWTA - (IMUX - OMUX). This does not turns in a remarkable loss of performance, as the results in [8] suggest.

However, if neither the frequency response of the *overall section* is known a priori, the dynamic pre-distortion can be performed based on the TWTA Profile only (red dashed lines). This further model simplification still improves link performance, but makes the waveform to loose robustness against group delay distortion. In other words, *the dynamic pre-distortion no longer has the channel equalization property*, and performance is sensibly dependent on the actual Symbol Rate. In this case, the channel equalization task is completely left at the demodulator.

3.2 Post Compensation Techniques

The effectiveness of pre-compensation techniques is sensibly dependent on the knowledge of the satellite channel characteristics, and the pre-distorted constellations are then optimised accordingly, as discussed in section 3.1. When the complexity at the receiver side, and hence the cost of the demodulator itself, is not a hard limitation, it is possible to design successful post-compensation algorithm which deal with the waveform distortion, due to channel non-linearity. This is the choice that Novelsat made for its professional demodulators NS2000 and modems NS3000. The actual algorithm implementation is proprietary, but we measured in laboratory the Total Degradation curves over ideal non linear channel for the post-compensated waveforms. This has been done using a couple of Novelsat modulator and demodulator, and according to the following procedure, which applies for both the DVB-S2 and the proprietary NS3 architectures:

1. select the MODCOD scheme,
2. decrease the noise level in the channel emulator until the demodulator locks,
3. assert that the QEF operation has been reached after 10^5 frames without errors.
4. measure the noise floor through the Signal Analyser, and hence the E_s/N_0 required over AWGN.
5. enable the non-linearity in the channel emulator, with a specific IBO and OBO.
6. repeat steps 2 and 3,
7. disable the non-linearity,
8. measure the noise floor through the Signal Analyser, and hence the C_{sat}/N.
9. evaluate D_{tot} using equation 2.3.

Figure 3.5 show the Total Degradation curves, which have been measured for three selected DVB-S2 MODCODs. In addition, a comparison is made with curves obtained in simulation, referring to the same performance over AWGN, measured with the demodulator of Novelsat. In particular, we seek to evaluate the effectiveness of Novelsat *Non Linear Mode*® against non-compensated and dynamically pre-distorted waveforms, over ideal non-linear channel. First, with reference to Figures 3.5a and 3.5b that an IBO of at least 0.5dB should be applied for safe operation, at least for high order MODCODs, like the ones with consider here.

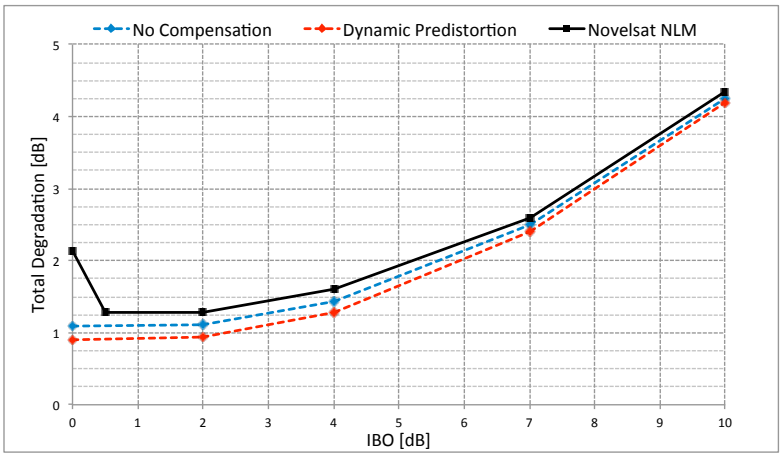

(A) 8PSK 5/6, Ref $E_s/N_0 = 9.39dB$

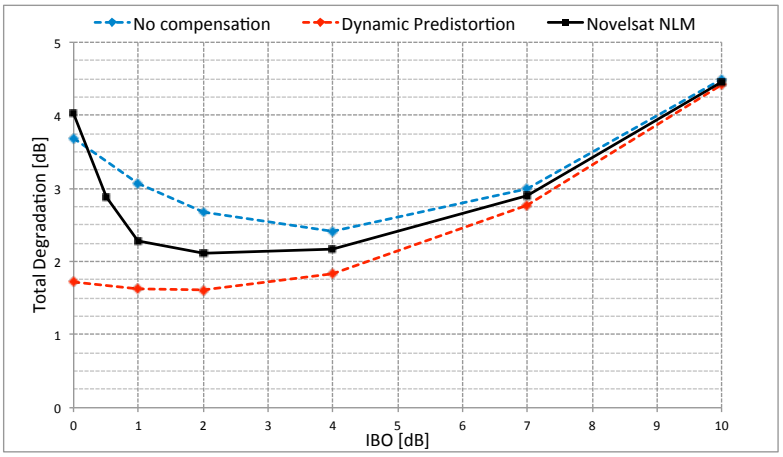

(B) 16APSK 2/3, , Ref $E_s/N_0 = 9.19dB$

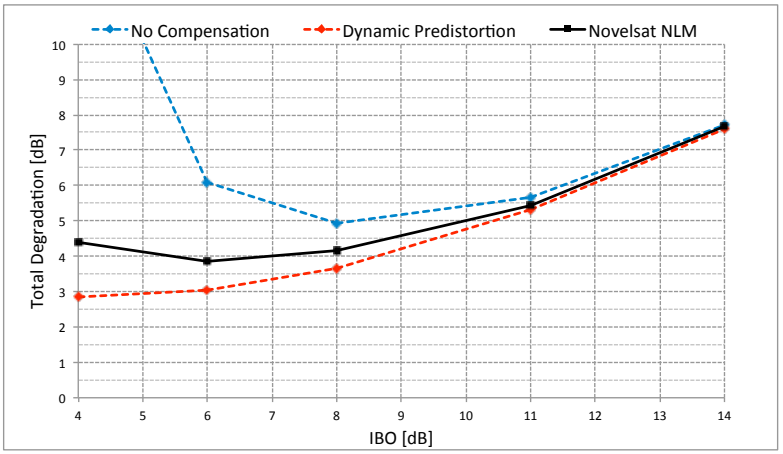

(C) 32APSK 3/4,, Ref $E_s/N_0 = 12.90dB$

FIGURE 3.5: Novelsat DVB-S2, Non Linear Mode Total Degradation over ideal Non Linear Channel (black lines), versus Total Degradation for non compensated and dynamically pre-distorted waveforms (blue and red dashed lines).

As known, waveforms with constant envelope, like the PSK modulated ones, are inherently robust against channel non-linearities, and the TWTA on board the payload can be driven close to saturation. In this case the pre-compensation yields only a slight improvement on link performance. On the other hand, it turns out here that the same does not apply for the post-compensation, since the curve measured for 8PSK 5/6 is only approaching the reference one (no compensation).

The effectiveness of Novelsat post-compensation becomes more and more evident for APSK constellations. In the case of 16APSK 2/3, the *Non Linear Mode*® is able to flatten the total degradation in the region between IBO 2dB and 4dB, with a non negligible gain, altought being only half the one achieved by pre-distortion. However, the post-compensation shows its best with 32APSK (and possibly higher, see NS3 features). Still it doesn't reach the performance pre-distorted waveforms have, but it enables reducing considerably both the Total Degradation and the optimum back-off, *without requiring any ad-hoc tuning*, and *without increasing the OBO at the TWTA output.*

In conclusion, altought pre-compensating remains the most attractive solution for breaking down Link Degradation, due to channel impairments, post-compensation techniques may in turn produce remarkable results. We stress that in this case no knowledge is supposed a priori on the channel characteristics, as in the case of pre-compensation techniques, where the waveform needs to be optimized offline for each operational condition.

Chapter 4

Multi Carrier per Transponder

The Single carrier per transponder configuration, discussed in chapter 2, is typically suitable for applications where a single carrier bears one or more data streams, which were multiplexed in a single earth station. These include digital video broadcasting, internet data trunking, and interactive broadband applications (forward link). On the other hand, the capacity of a particular transponder may be shared by different uplinks. This is the case when multiple earth stations access the same transponder, being placed possibly anywhere within the satellite coverage. As a consequence, the problem of multiple access to the satellite channel arises [1, Chapter 6]. In this chapter we analyse the challenges to be addressed in the classic Frequency Division Multiple Access (FDMA), where a dedicated carrier is associated with each uplink. The FDMA is often preferred in practice, because it does not require synchronization between remote earth stations.

4.1 Intermodulation products

It was seen in section X that the satellite channel has a non-linear transfer characteristic. Being a transparent repeater, it simultaneously amplifies all the carriers which lie in the channel pass band, at different frequencies. In general, when N sinusoidal signals at frequencies $f_1, f_2 \ldots, f_N$ pass through a non-linear amplifier, the output contains not only the N signals at the original frequencies but also undesirable signals called *intermodulation products*. These appear at frequencies f_{IMX} which are linear combinations of the input frequencies:

$$f_{IMX} = m_1 f_1 + m_2 f_2 + \ldots + m_N f_N, \tag{4.1}$$

where $m_1, m_2, \ldots, m_N$ are positive or negative integers.

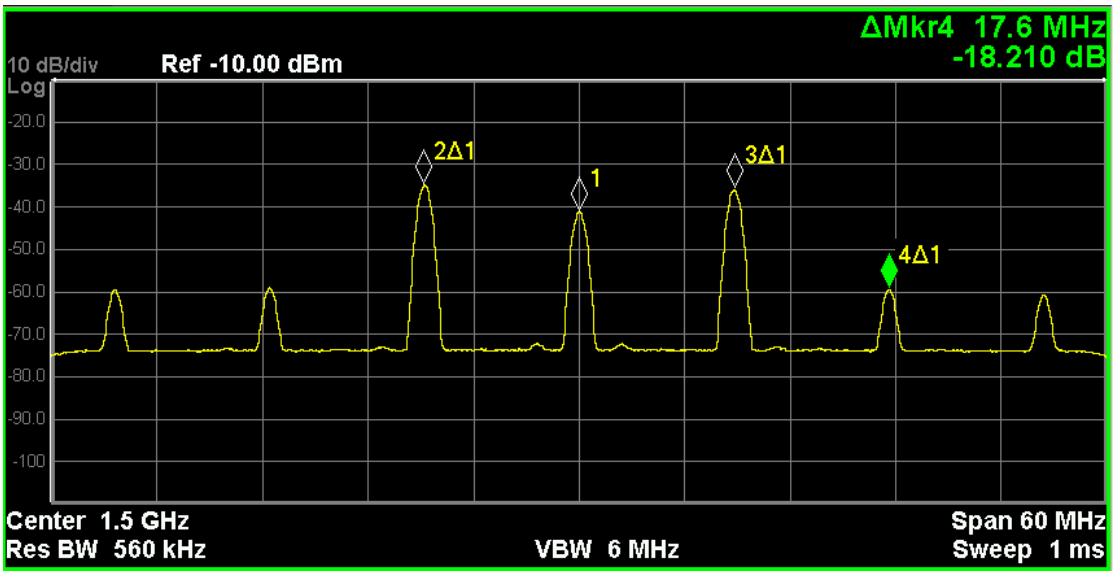

FIGURE 4.1: Intermodulation products

The quantity $X = |m_1| + |m_2| + \ldots + |m_N|$ is called the order of an intermodulation product. When the center frequency of the passband amplifier is large compared with its bandwidth, which is always the case for a satellite repeater channel (compare the center frequency of several GHz to the bandwidth of a few tens of MHz), only the odd intermodulation products, where $\sum m_i = 1$, fall within the amplifier bandwidth. Moreover, the amplitude of the intermodulation products decreases with the order of the product. Hence, in practice, only products of order 3, and to a lesser extent 5, are significant. It can be seen that, in the case of unmodulated carriers of unequal amplitude, the intermodulation products are greater at high frequencies if the carrier of greater amplitude is that which has the higher frequency and at low frequencies if the carrier of grater amplitude is that which has the lower frequency. This indicates the advantage of locating the most powerful carriers at the extremities of the channel bandwidth, as the corresponding most powerful intermodulation products then fall out of channel bandwidth, and do not propagate on the downlink [1, Chapter 6]. This is because of the cut off effect of the OMUX filter, which is placed on the payload, after the TWTA.

4.1.1 The Carrier to Intermodulation Noise ratio

When the carriers are modulated, the intermodulation products are no longer spectral lines, and their power is dispersed over a spectrum which extends over a band of frequencies. The higher the number of carriers, the more the superposition of the spectra of the intermodulation products leads to a spectral density which is nearly constant over the

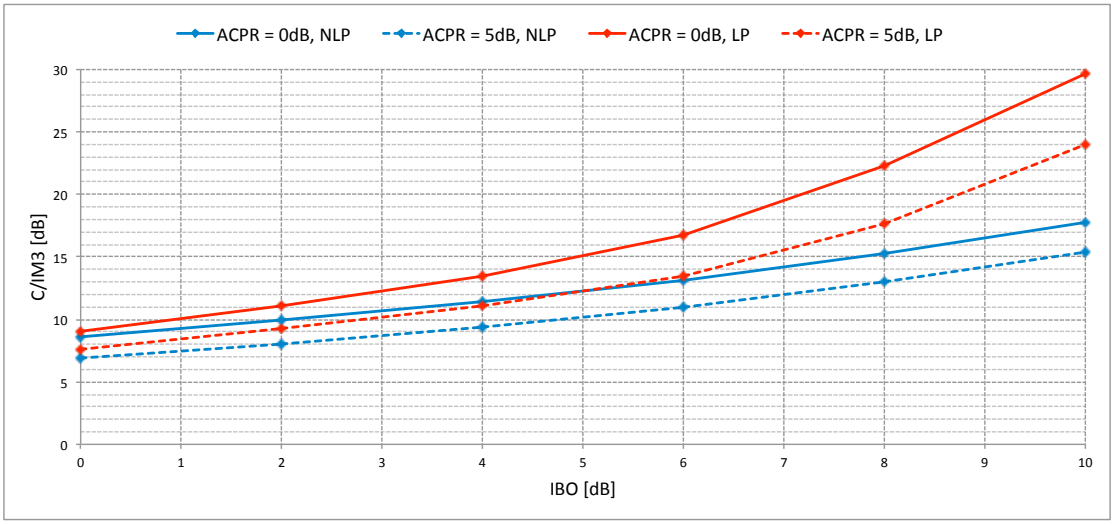

FIGURE 4.2: Carrier to Intermodulation ratio. CS = 9.6MHz

whole of the amplifier bandwidth, and this justifies considering intermodulation products as white noise. In view of this, the Satellite Operator recommends the minimum carrier to intermodulation noise ratio for a given back-off level, in order to limit the impact of intermodulation noise on the overall carrier to noise ratio, at the receiver side. This can be conveniently quantified through lab measures.

Figure 4.1 shows the generation of intermodulation products from three unmodulated carriers. These were observed in laboratory in L-band. The central carrier was allocated at $f_2 = 1500$MHz, and the two side ones were equally spaced by either 8.8MHz ($f_1 = 1491.2$MHz, $f_3 = 1508.8$MHz) or 9.6MHz ($f_1 = 1490.4$MHz, $f_3 = 1509.6$MHz). It turned out that the frequency of the intermodulation product of order 3 is $f_{IM3} = 1500 \pm 17.6$MHz or $f_{IM3} = 1500 \pm 19.2$MHz respectively, which equals calculating 4.1, with $m_1 = -1$, $m_2 = m_3 = 1$. This case study is aimed to the prototype configuration of three modulated carriers all having the same symbol rate of 8Mbaud and SRRC shaped with a roll-off factor of 10% or 20%, which are amplified through the same repeater channel, as we shall analyse later.

With reference to Figure 4.1, we measured the carrier to intermodulation noise ratio as the delta in dB between the peak of the internal carrier and the peak of the intermodulation product of order 3, or IM3. The measure has been carried out in both the cases in which all the carriers have the same power, and when the two side ones are greater by 5dB. The latter is of interest, since allocating the most powerful carriers at the extremities of the channel bandwidth allows filtering out the greatest intermodulation products by the OMUX, thus avoiding cross system interference (as discussed above), but the inner carrier(s) C/N is subject to a more important degradation.

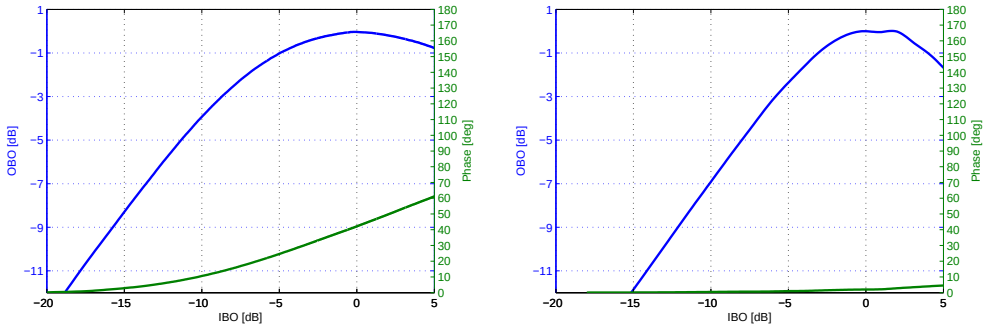

(A) Non Linearised Profile (B) Linearised Profile

FIGURE 4.3: TWTA prototype profiles, AM/AM and AM/PM characteristics

The power associated with intermodulation products in the downlink depends on the AM/AM characteristic of the TWTA on board the payload. The more the latter is linear, the lower the impact of intermodulation noise on the overall link quality. In [4] two prototype TWTA profiles were introduced, as sketched in Figure 4.3. The Non Linearised Profile of 4.3a had already been considered in Chapter 3, as a worst case scenario. In this chapter we present a serie of simulations and measures which has been carried out with reference to both profiles. This is because the only way to combat intermodulation noise is to have the more linear possible TWTA transfer characteristic.

4.2 Total Link Degradation

In multi carrier per transponder, intermodulation noise is the predominant channel impairment. The Total Link Degradation can still be evaluated by 2.3 and 2.5. We performed a serie of simulations, using a procedure similar to the one outlined in section 2.2.2, but adapted to the multi carrier scenario, as well as a serie of lab measures on Novelsat professional modems. The are several possible configurations to consider as case study, which depend on:

- number of carriers,
- symbol constellation,
- link performance over AWGN,
- profile of channel non-linearity,
- carrier spacing,
- roll-off factor,

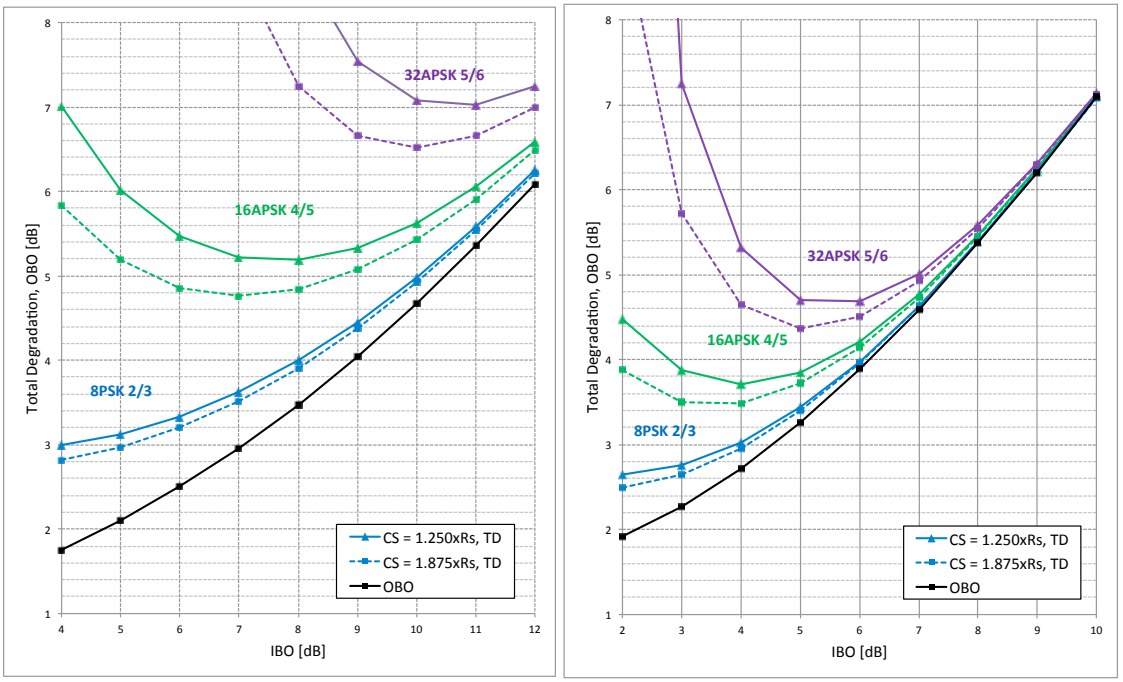

(A) Non Linearised Profile

(B) Linearised Profile

FIGURE 4.4: Total Link Degradation over Non Linear Channel. 3 carriers, ACPR = 0dB, Symbol Rate = 8Mbaud, Roll-Off = 20%. IBO values referred to the aggregate power.

- adjacent channel power ratio (ACPR).

As a consequence, one has to seek for some prototype cases, whose study shall yield possibly general results. The choice here is to consider different configurations based on three carriers, Symbol Rate 8Mbaud, and both the TWTA profiles of Figure 4.3.

4.2.1 Simulations

Consider the Total Degradation curves of Figure 4.4. These have been obtained in simulation, and quantify the link degradation over non-linear channel, for different DVB-S2 MODCODs. We chose the 8PSK 2/3, 16APSK 4/5 and 32APSK 5/6, as representatives of the MODCODs available in [4] and listed in table 2.2. In addition, it is assumed here that all carriers have the same power i.e. ACPR = 0dB, and the IBO level is referred to the aggregate power. We observe what follows:

1. the link degradation is in general more important than in the case of single carrier per transponder, due to intermodulation noise. This applies in particular for the Non Linearised profile.

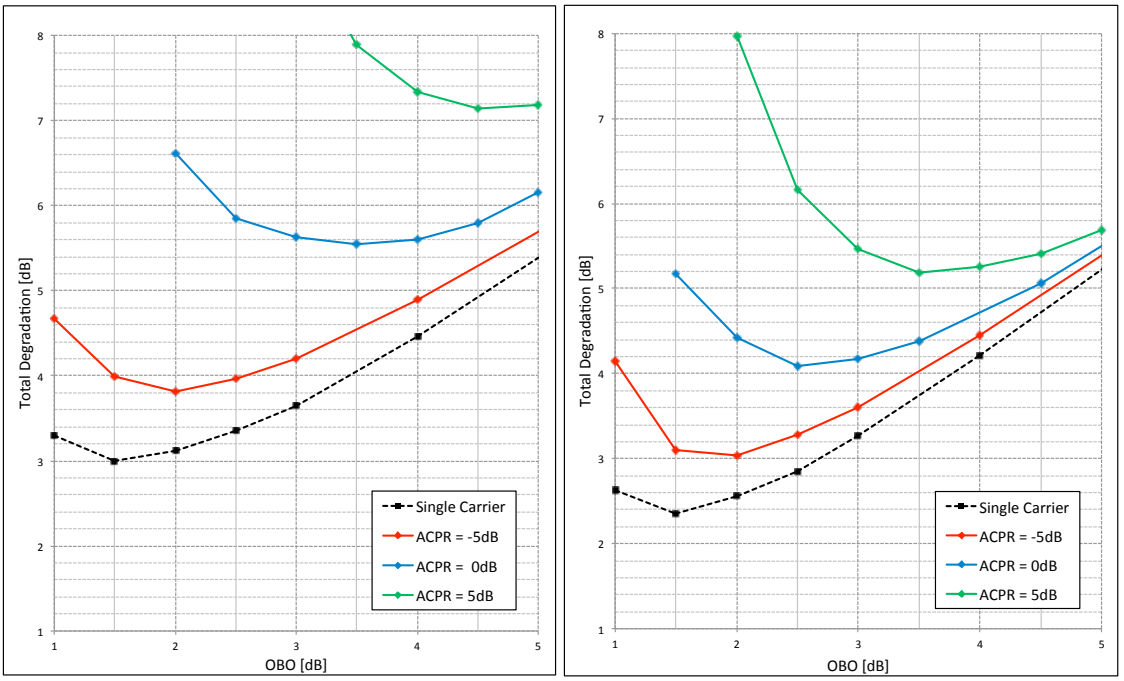

(A) Non Linearised Profile (B) Linearised Profile

FIGURE 4.5: Total Link Degradation over Non Linear Channel, Novelsat NS3 16APSK 4/5. 3 carriers, Symbol Rate = 8Mbaud, Roll-Off = 20%, CS = $1.2\times R_s$. OBO values referred to the aggregate power.

2. Increasing the carrier spacing yields a gain only up to 0.5dB on link degradation, at the optimum back-off, at the price of a very inefficient use of the channel capacity. This is because an higher carrier spacing *turns away* the frequency of IM3, but intermodulation noise spreads over a range of frequencies large enough to vanish the effect of spacing.

3. The link degradation due to the TWTA Linearised profile is resolutely lower than the one associated with the Non Linearised profile, and the optimum back-off is closer to saturation.

4.2.2 Lab Measures

In general, the carriers allocated into a certain satellite channel do not necessarily have the same power at the TWTA input. As a consequence, intermodulation noise impacts more the carriers with the lower power, since it depends on the aggregate power of the input section. The quantity which measure the difference in dB between the power of adjacent information channels is the Adjacent Channel Power Ration (ACPR). Here we focus on the prototype case in which the power the central carrier is either 5dB lower (ACPR = 5dB), at the same level (ACPR = 0dB) or 5dB higher (ACPR = -5dB) than the two adjacent channels power.

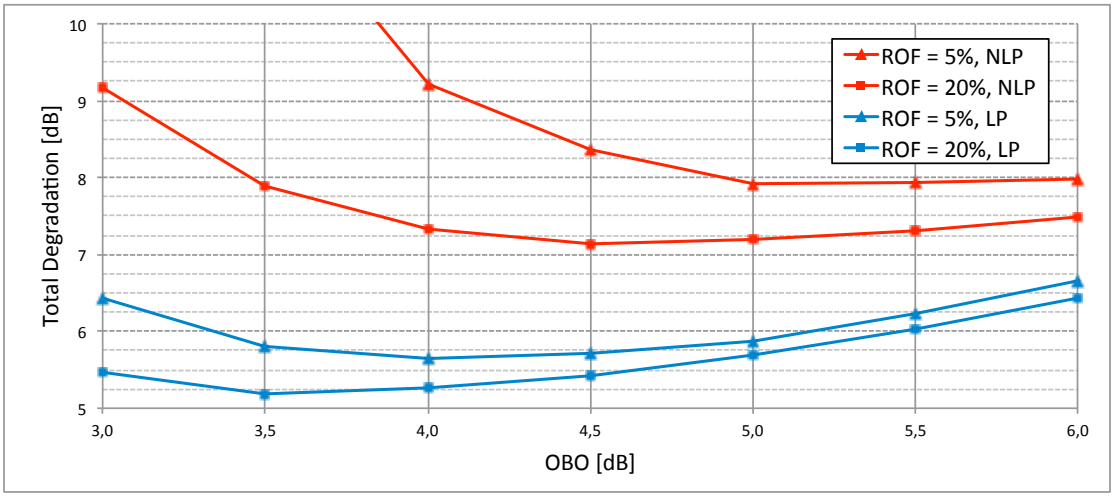

FIGURE 4.6: Total Link Degradation with minimum carrier spacing, Novelsat NS3 16APSK 4/5. $CS = R_s \times (1 + \rho)$, ACPR = 5dB

Figure 4.5 shows the total degradation measured for the differents ACPRs with the Novelsat modems introduced in section 3.2, and are meant for the NS3 System Architecture, using the 16APSK 4/5. The performance over AWGN of the latter had been quantified in $[E_s/N_0]_{req} = 10.86dB$ (against the 11.03dB of the DVB-S2 specifications). In particular, with reference to Figure 4.5a, notice that when the ACPR is equal to 5dB, the optimum OBO becomes as high as 4.5dB, and the Total Degradation exceeds the threshold of 7dB. In other words, under certain condition, the link can become impractical for the higher order MODCODs. Hence, the linearity of the TWTA is critical in order to allow a certain flexibility on the transponder configuration.

The DVB-S2 specifications provide only three different roll-off factors for the shaping filters. These are $\rho = 35\%$, 25% and 20% respectively. However, in recent times, within the discussion about the future of satellite communication technologies, the industry have been wondering if it is feasible to introduce lower roll-offs, in order to exploit the space segment more efficiently, by reducing the excess bandwidth of information channels and hence the spacing between adjacent carriers. Some modem manufacturers, like Novelsat does, started to provide roll-offs down to 5%. Unfortunately, the gain in the efficiency on the spectrum utilisation is to be paid by an increase of ISI at the decision point, as the pulse shapes with lower roll-offs are more sensible to the waveform distortion. In addition, recall that by reducing the carrier spacing, one increases the intermodulation noise. Figure 4.9 approaches the results introduced in 4.5, for the case of roll-off = 20%, with some equivalent ones related to roll-off = 5%. Note that both the optimum OBO and the corresponding total degradation increase up to an extra 0.75dB roughly. Considering the one for the TWTA Non Linearised profile, and being these measures taken for the case ACPR = 5dB, we declare that curve as the most critical one in the serie.

4.3 Adjacent Channel Interference

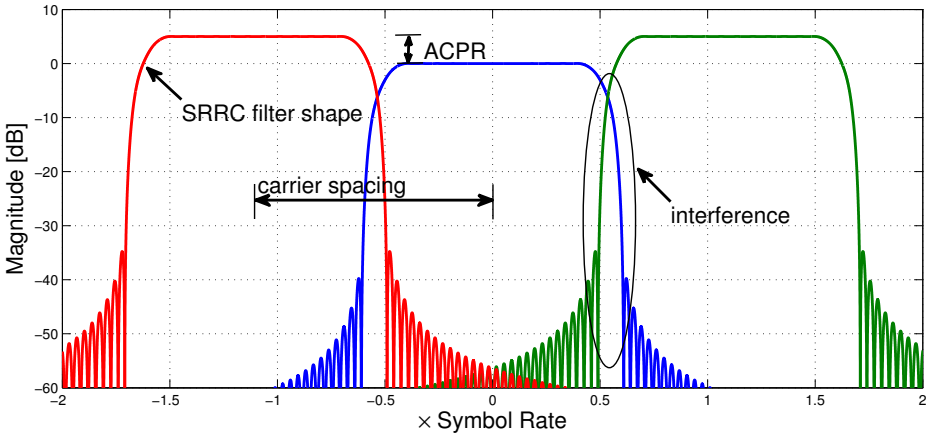

FIGURE 4.7: Pictorial view of quantities involved in adjacent channel interference

In section 4.2.1 we saw that increasing the carrier spacing CS is not an efficient countermeasure to combat the link degradation due to intermodulation noise. The latter is strongly dependent on the type of channel non-linearity, as shown in Figure 4.4. Hence, given a certain TWTA profile, one may consider improving at least the transponder passband utilisation, by approaching in frequency adjacent information channels.

The carrier spacing reduction can even be such that $CS/R_s < 1 + \rho$, i.e. the spectral content of adjacent information channel can partially overlap. This involves a certain amount of inter system interference, since a part of the energy of a channel falls in the band of frequencies of the adjacent one, and vice versa.

Interference turns into ISI at the decision point, and further lower the robustness of the system against noise, as all other channel impairments do. It can be shown that the ISI due to inter system interference is in turn gaussian, with variance I, and can still be thought as an additional noise term. Hence, with analogy to what done in section 2.1, we can thus consider the quantity $D_{extra} = [1 + I/N]$ which determines the link quality degradation due to interference, and depends now on the normalised carrier spacing CS/R_s, roll-off factor ρ, and adjacent channel power ratio ACPR. Here we choose to refer such degradation to the link performance over non-linear channel, in multi-carrier configuration and with $CS/R_s = (1 + \rho)$, rather than to the performance over AWGN. This is why we call it Extra Degradation. Figure 4.8 shows some simulation results which are meant for the TWTA Linearised Profile, roll-off 20%, and selected MODCODs and ACPR. Notice that even when the overlap is as high as the 10% of total channel bandwidth, the extra degradation does not exceed the threshold of 1dB for the DVB-S2 APSK MODCODs, provided the ACPR is lower than 3dB. When the contrary applies,

then the impact of interference becomes more critical, and the normalised spacing should only be reduced to a lesser extent.

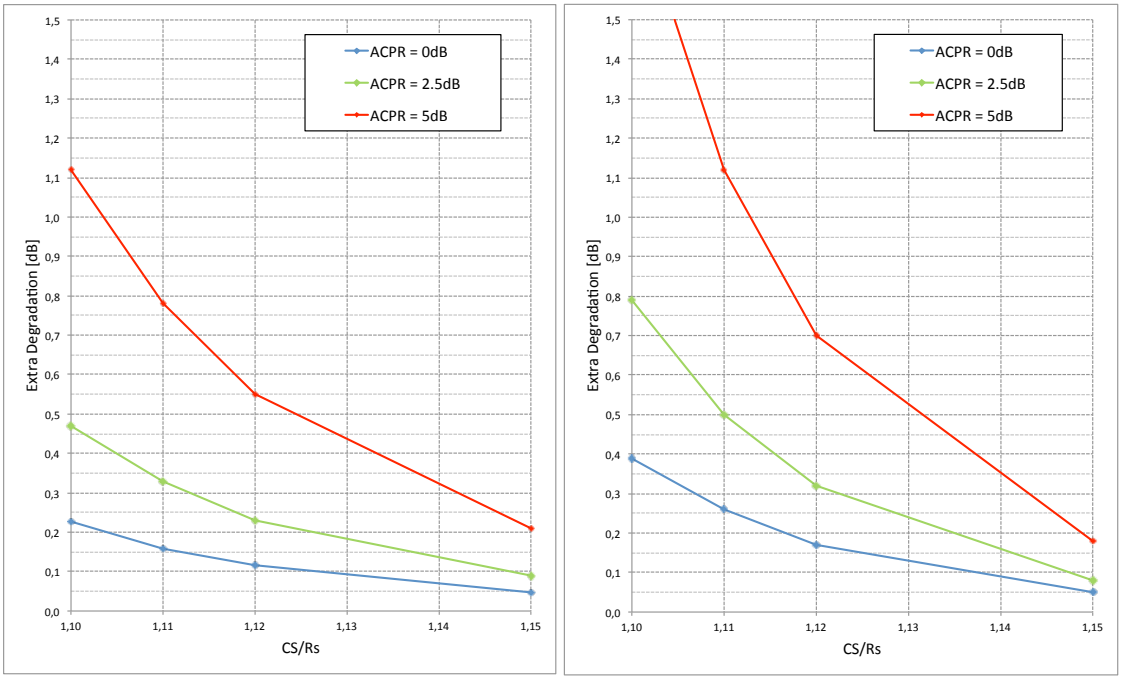

(A) 16APSK 4/5. IBO 4dB, OBO 2.7dB (B) 32APSK 5/6. IBO 6dB, OBO 3.9dB

FIGURE 4.8: Extra degradation due to adjacent channel interference, TWTA Linearised Profile. OBO values referred to the aggregate power.

4.3.1 Modems Filters Validation

Modems available in both the consumer and the professional market perform SRRC pulse shaping at both the transmitter and receiver sides, as suggested in [4]. However, the actual pulse shape implementations and the consequent signal spectrum may not be compliant with the relative specification masks, as discussed in Appendix C, due to hardware limitations. This is particularly likely for the newly introduced lower roll-offs down to 5%. Note that the transmit pulse shape can be verified by introducing a spectrum analyser ad the modem output, but there is no direct way to validate receive one. The latter should be identical to the transmit pulse, but it turns out that it is not always the case, for every modem manufacturer. It can happen that the receive SRRC filter is designed with a larger roll-off than the one with which the transmitted waveform is shaped. As a consequence, when limiting the carrier spacing, a larger interference is caught at receiver side, from the adjacent information channels.

Figure 4.10 shows the measured link degradation due to interference for both the Novelsat and Workmicrowave professional modems, considering roll-offs lower than or equal to the 20%. Note that here the aim to verify the transmit and receive filters shape,

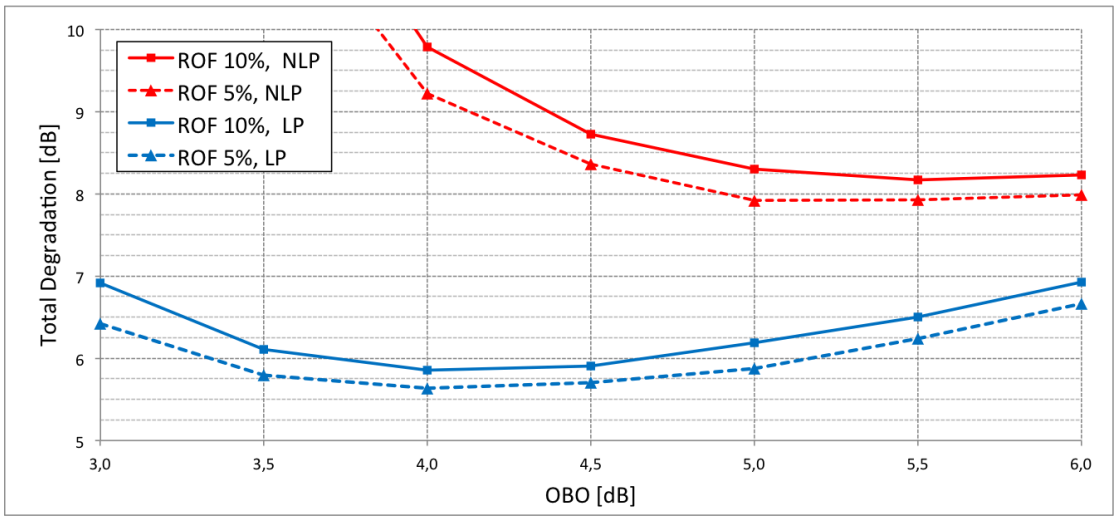

FIGURE 4.9: Total Link Degradation with reduced carrier spacing, Novelsat NS3 16APSK 4/5. $CS/R_s = 1.05$, ACPR = 5dB

and the degradation is simply referred to the performance over AWGN. In addition, an ACPR as high as 5dB is considered, to emphasise the impact of interference.

Notice that Novelsat provides roll-offs of either 20%, 15%, 10% and 5% (blue lines). As expected, the impact of interference becomes non negligible (say higher than 0.2dB) only when the normalised carrier spacing is reduced *well beyond* the nominal value of $CS/R_s = 1+\rho$. On the other hand, Workmicrowave only provides roll-offs of either 20% or 5% (red lines). Here, we found a results comparable to the relative ones obtained for Novelsat only in the case of roll-off 20%. When applying the roll-off 5%, the degradation curve is only comparable to Novelsat 15%. We concluded that, even if the transmit pulse is really with roll-off 5%, as we verified in lab, the receive one is evidently larger, and the actual carrier spacing on an eventual uplink shall not be lower than $1.1 \times R_s$.

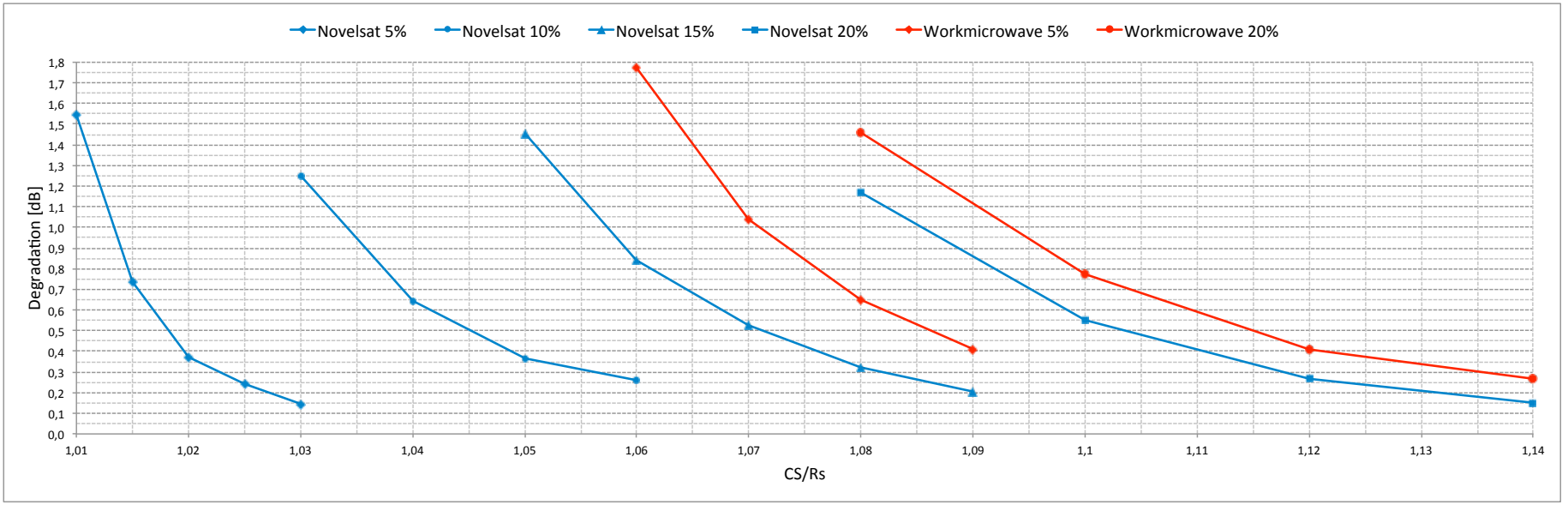

FIGURE 4.10: Link degradation due to ACI. Novelsat NS3 vs Workmicrowavre DVB-S2, 16APSK 4/5. ACPR = 5dB

4.4 final considerations

Multi carrier per transponder configurations enable a wide range of applications, particularly suited for the professional market. For instance, consider the case in which the satellite access provider want to give internet access to different customers, located in remote sites. The solution which is typically adopted is to multiplex the forward link on a common carrier, and allocating a different carrier for each return channel, according to the FDMA scheme. Since the transponder pass bands are of fixed sizes, of the order of several tens of MHz this inevitably introduce the multi carrier scenario, with the challenges we discussed so far.

The satellite end to end link quality is subject to several factors which depend on both meteorological and cosmological factors, which directly impact the carrier to noise ratio at receiver side. The DVB-S2 introduced the Adaptive Coding and Modulation concept, aimed at varying the transmitted MODCODs depending on the actual SNR at the decision point. This is achieved by proper signalling though the return channel, and for each different remote user [4].

The satellite channel has typically a non-linear behaviour, as we widely discussed in these pages, and for a given TWTA profile the optimum back-off is MODCOD dependent. However, power levels on the uplinks cannot be varied on a dynamic basis, as the maximum aggregate power at the TWTA input is limited by the amplifier saturation. Thus, power back-offs can only be setted a priory, for a specific multi-carrier configuration, as an average of the optimum levels associated with the MODCODs involved in the ACM.

Due to intermodulation noise, back-off levels shall in general be considerably lower than the ones applicable to the single carrier per transponder scenario (see Table 2.2). The pre compensation techniques discussed in Chapter 3 deal with the waveform distortion due to channel non-linearity at low back-offs. Since here each carrier alone feed the amplifier in a quasi linear zone, these techniques fail in reducing the Total Link Degradation, which is indeed dominated by intermodulation. In conclusion in this case the TWTA linearity is the most important factor which enables the use of higher constellation orders like the APSK, and thus increases the average spectral efficiency, in the perspective of ACM.

Appendix A

The Simulation Environment

A.1 General approach

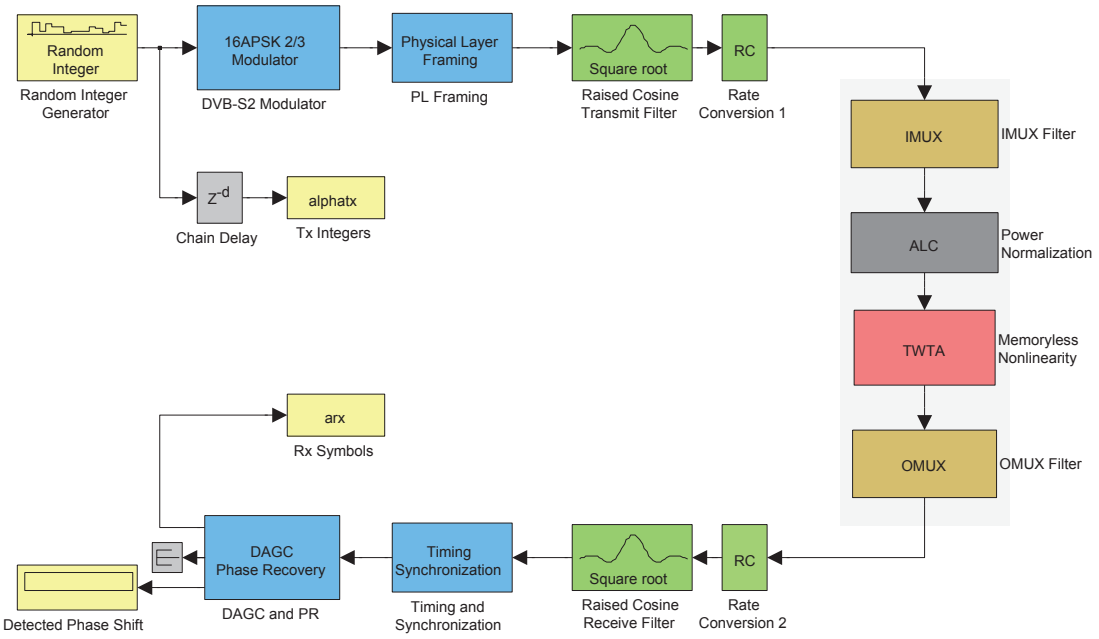

FIGURE A.1: Simulink Block Diagram

All the simulations presented in this work have been carried out in Matlab and Simulink. In particular we chose to build Simulink block diagrams (like the one in Figure A.1) for generating DVB-S2 compliant baseband waveforms, as well as a model for a 36MHz transponder. The purpose of the simulations is to quantify the distortion the waveform undergoes in a typical satellite channel, due to channel impairments. This turns into ISI and constellation warping, at the demodulator side. The latter depend on several parameters, as discussed in Chapters 2 and 4. As a consequence, Simulink block-diagrams shall be run iteratively, by varying those parameters which are of interest for a specific

case study. This is better achieved through Matlab scripts, which are meant for configuring, running and collecting output signals from a block-diagram. In conclusion, the general procedure we adopted involved first creating a proper Simulink block-diagram, for the case study of interest, and subsequently writing a Matlab script to manage the block-diagram execution.

A.2 Simulink custom blocks

The Simulink environment provides natively a rich library of blocks which are ready to be used for the construction of block diagrams. However, often one needs to implement ad-hoc blocks for some specific purposes. As an example, Matlab/Simulink only provide bit-mappers into QAM or PSK symbol constellations. Since here the interest is on both the PSK and the APSK constellation introduced in [4], we needed to build our own custom blocks for bit-mapping and soft demodulation for these constellations. This has been done though Matlab Function Blocks, i.e. Simulink blocks that directly contain Matlab code. Mathworks suggests to use built in blocks when possible, to create custom subsystems which are more efficient and hence of faster execution at runtime. This is the solution we adopted for modelling a channel non-linearity.

A.2.1 modelling a general memoryless non-linearity

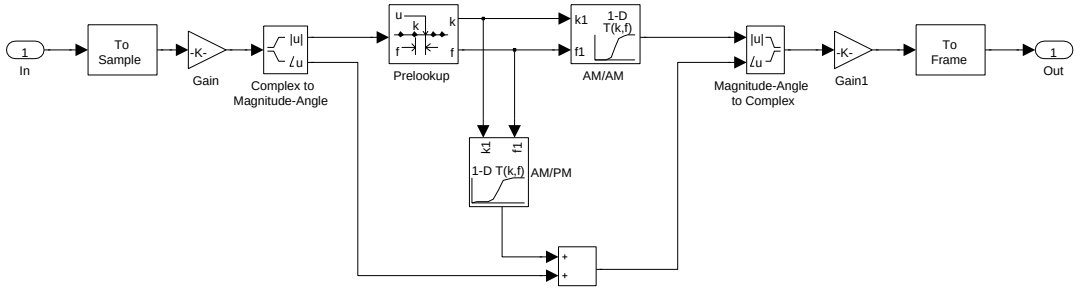

FIGURE A.2: Memoryless non-linearity Simulink model.

As discussed throughout this work, the satellite channel impairments are dominated by the non-linearity introduced by the TWTA on board the payload. This is well described by the AM/AM and AM/PM curves and can be conveniently modelled by mean of interpolated look-up tables. Figure A.2 shows the memoryless non-linearity subsystem which has been included in the simulations. The subsystem requires the transfer curves to be given in form of breakpoints for both input and output quantities. The smaller the step the better, even if the model proved to work properly even with linearly interpolated

breakpoints spaced by 1dB. From left to right, the tasks performed by the subsystem of Figure A.2 are as follows:

1. Apply an IBO to the input signal, which is supposed to have unit power at the subsystem input.
2. Split the complex input signal into its magnitude and phase.
3. Perform a pre look-up on the signal magnitude. The pre look-up block calculates the index and interval fraction that specify how its input value relates to the breakpoint data set. This is achieved by linear interpolation.
4. Feed the AM/AM and AM/PM look-up tables with the output of the pre look-up. This reduces the computational burden that one would have, using two independent tables.
5. Add the phase shift to the original signal phase
6. Recombine magnitude and phase signal into the final output
7. Eventually apply an output scaling (not used).

Altough it is not the only possible implementation, our solution is flexible in the sense that with look-up tables one may model whichever non-linearity profile, possibly measured though IOT (In Orbit Testing). For the purposes of this work we referred to the general TWTA Non Linearised and Linearised profiles, as introduced in Chapter X.

Appendix B

Lab Measures

The lab measures presented in this work have been done using a couple of Novelsat or Workmicrowave professional modems. The multicast traffic was generated by iperf (iperf.sourceforge.net), and chosen to be of UDP type, with packet length 188KB (standard length of MPEG transport stream packets). The modems connected through a satellite channel emulator (DCS3020, www.izt-labs.de) which can deal with signal bandwidth as large as 36MHz. The emulator can add white noise over a band of 60MHz, some fading profile variable over time, a memoryless nonlinearity, as well as some shaped noise, phase noise and more. E_s/N_0 values have been measured by an Agilent Signal Analyser (N9010A, www.agilent.com), using the Adjacent Channel Power (ACP) feature. This gives the difference in dB between the power measured integraging the PSD on different bands. Typically one may integrate over the same bandwidth both the power in band and the noise floor out of band. This yields the ratios

$$\left[\frac{C+N}{N}\right] \Rightarrow \left[\frac{C}{N}\right] = \left[\frac{C+N}{N}\right] - 1. \tag{B.1}$$

B.1 Performance over AWGN

Modems commercially available on the professional and consumer market both implement one or more System Architectures. These can be either a standardised technology or a proprietary solution. In the first case, one expects that given a certain MODCOD, performance in term of E_s/N_0 required for QEF over AWGN match the reference ones indicated in the standard itself, which normally are achieved by computer simulations in ideal conditions at the demodulator side. When instead a proprietary solution is adopted, performance is directly declared by the manufacturer. However, it turns out

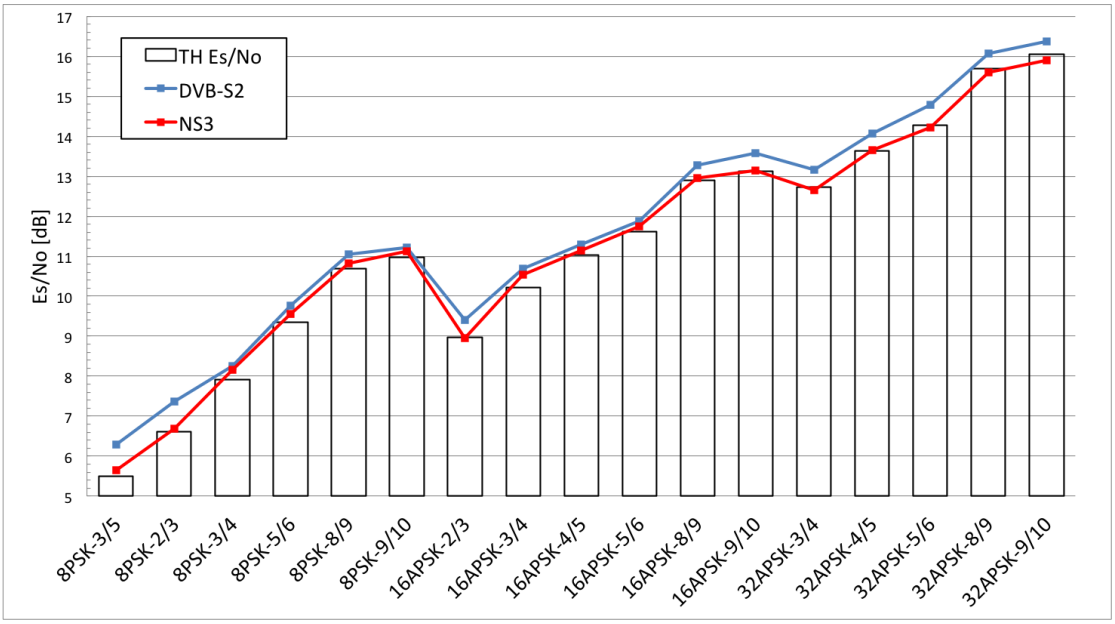

FIGURE B.1: Novelsat DVB-S2 and NS3 performance over AWGN, versus ETSI specifications.

that especially in the case of implementations of standards, the actual performance of the device deviate from the expected theoretical ones. Figure B.1 shows the performance measured over AWGN for Novelsat modems, for both the standard DVB-S2 and proprietary NS3 (only MODCODs available also in the DVB-S2 specs are considered here). Notice that DVB-S2 measured E_s/N_0 for QEF are between 0.25dB and 0.8dB higher than the reference ones, while NS3 matches, and in some cases also slightly outperforms, the DVB-S2 theoretical performance.

But how do we measure the performance of a link in terms of E_s/N_0 for QEF? According to the definition given in [4], the system operates in QEF conditions when the Packet Error Rate at receiver side is less than 10^{-7}. In practice, determining the QEF point in a lab experiment means running a transmission session of at least 10^7 packets, which already requires several hours depending on the spectral efficiency and hence on the MODCOD. In addition also the packet length influences the time needed. We chose to refer to the Frame Error Rate instead, because the frame length in DVB-S2 systems is fixed (only normal frames of 64800 bits have been considered here). We limited the transmission session to either 10^5 or 10^6 frames, in order to get results in a reasonable time elapse.

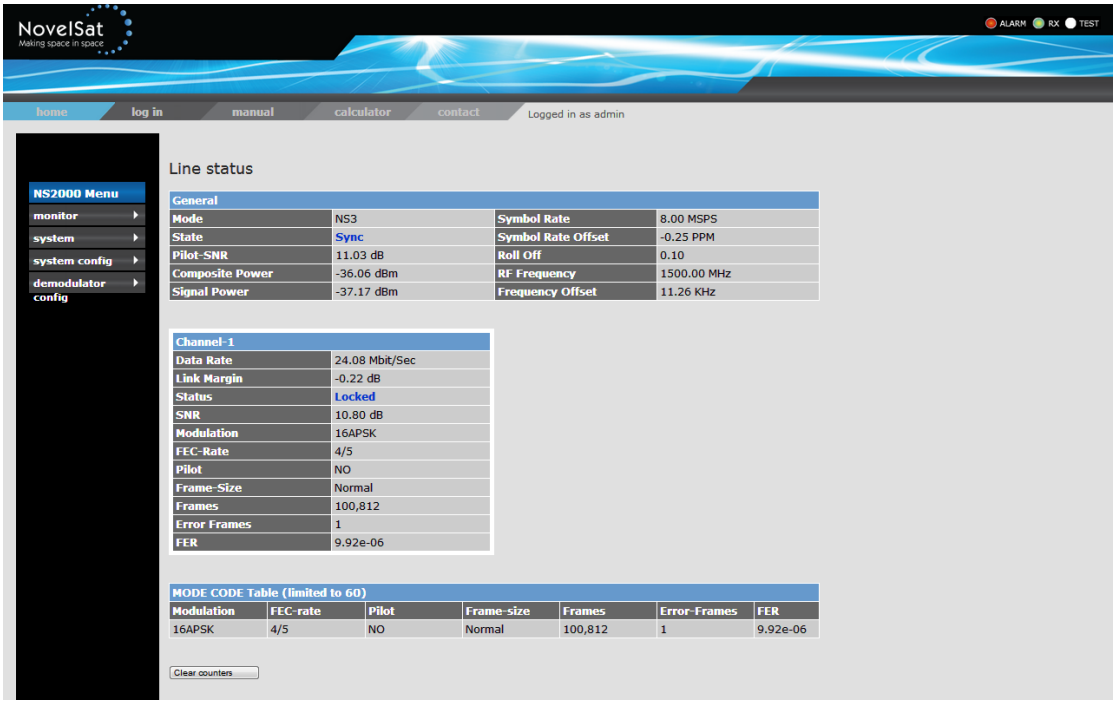

FIGURE B.2: Novelsat NS2000 demodulator, traffic monitoring.

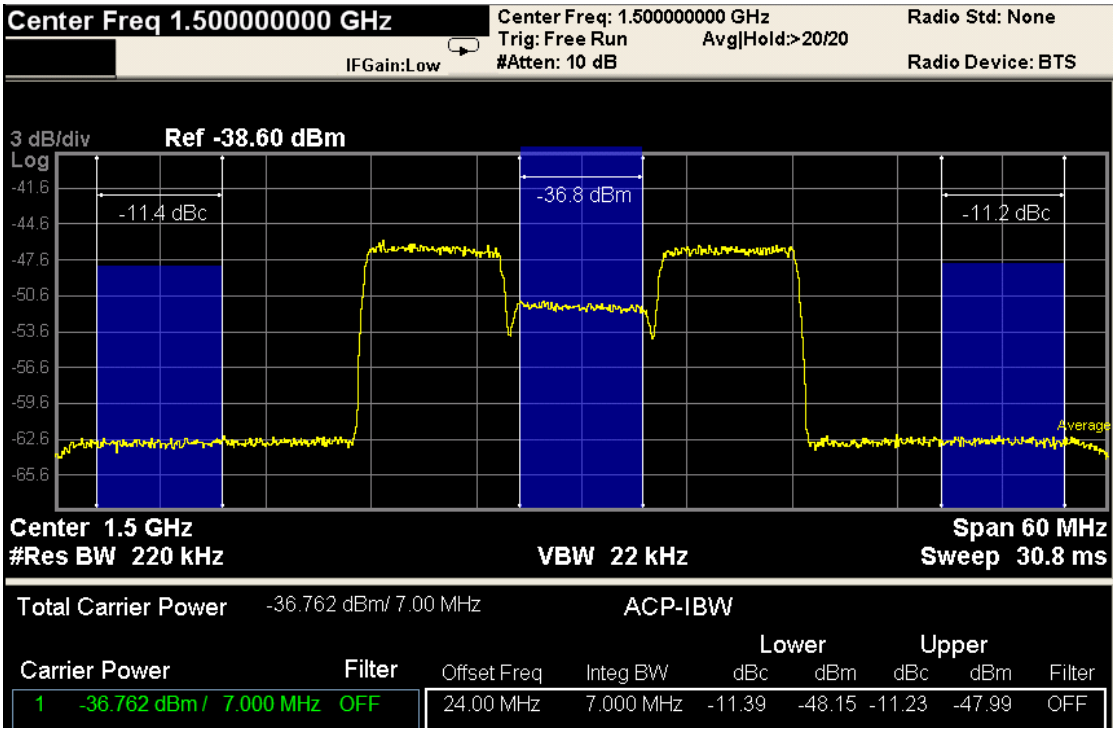

FIGURE B.3: Agilent N9010 Signal Analyzer, ACPR measures.

B.2 Channels with impairments

The typical satellite channel is far from being AWGN, but performance in the ideal case is the reference for quantifying the impact of channel impairments. Suppose for instance to transmit an APSK modulated waveform with power such that the TWTA in orbit is driven close to saturation. Then the distortion due to non-linearity, i.e. constellation warping and ISI, lower the noise level which is acceptable for QEF in the AWGN channel. Hence, once reached more than 10^5 frames without error, we shut off the non-linearity from the channel emulator, and we measure the noise floor. This operation is necessary, because otherwise it would be difficult to evaluate the in band noise floor, since it is masked by the signal spectral regrowth. It turns out that the E_s/N_0 measured on the channel with impairments is always greater than the one over AWGN. The difference in dB between the two, plus the back-off applied, constitutes the Total Link Performance Degradation (see also section 2.2.1).

Appendix C

SRRC Filters

Any digital communication system shall provide the waveform a proper baseband filtering both in transmission and in reception, in such a way that in a distortion free channel the overall system impulse response exhibits the Nyquist property for the absence of ISI [9, Chapter 7].

In practice, the choice often falls on the Square Root Raised Cosine (SRRC) filtering in both the transmitter and receiver side. In such a way, the overall system impulse response is of the Raised Cosine (RC) type, which indeed is of Nyquist. In the frequency domain, the baseband SRRC filters can be described by the theoretical function given by

$$H(f) = \begin{cases} 1, & \text{if } |f| < f_N(1-\rho) \\ 0, & \text{if } |f| > f_N(1+\rho) \\ \left\{ \frac{1}{2} + \frac{1}{2} sin \frac{\pi}{2 f_N} \left[\frac{f_N - |f|}{\rho} \right] \right\}^{1/2}, & \text{otherwise} \end{cases} \tag{C.1}$$

where $f_N = R_s/2$ is the Nyquist frequency and ρ is the Roll-Off factor. However, practical implementations are based on FIR or IIR digital filters, and the theoretical approximation is traded off with hardware complexity. The latter is determined by the number of filter coefficients, which in turn impacts the speed of the filtering process. In order to meet specific real time constraints, the solution based on IIR filters is generally adopted, since these require a lower number of coefficients to achieve a target quality of design.

On the contrary, straightforward implementations based on FIR filters, with a high number of coefficients, are suitable for the purpose of simulations. We chose a different number of taps for each filter Roll-Off, in a such a way to have all filter designs approximating the theoretical shape of C.1 with a comparable quality. It turns out that

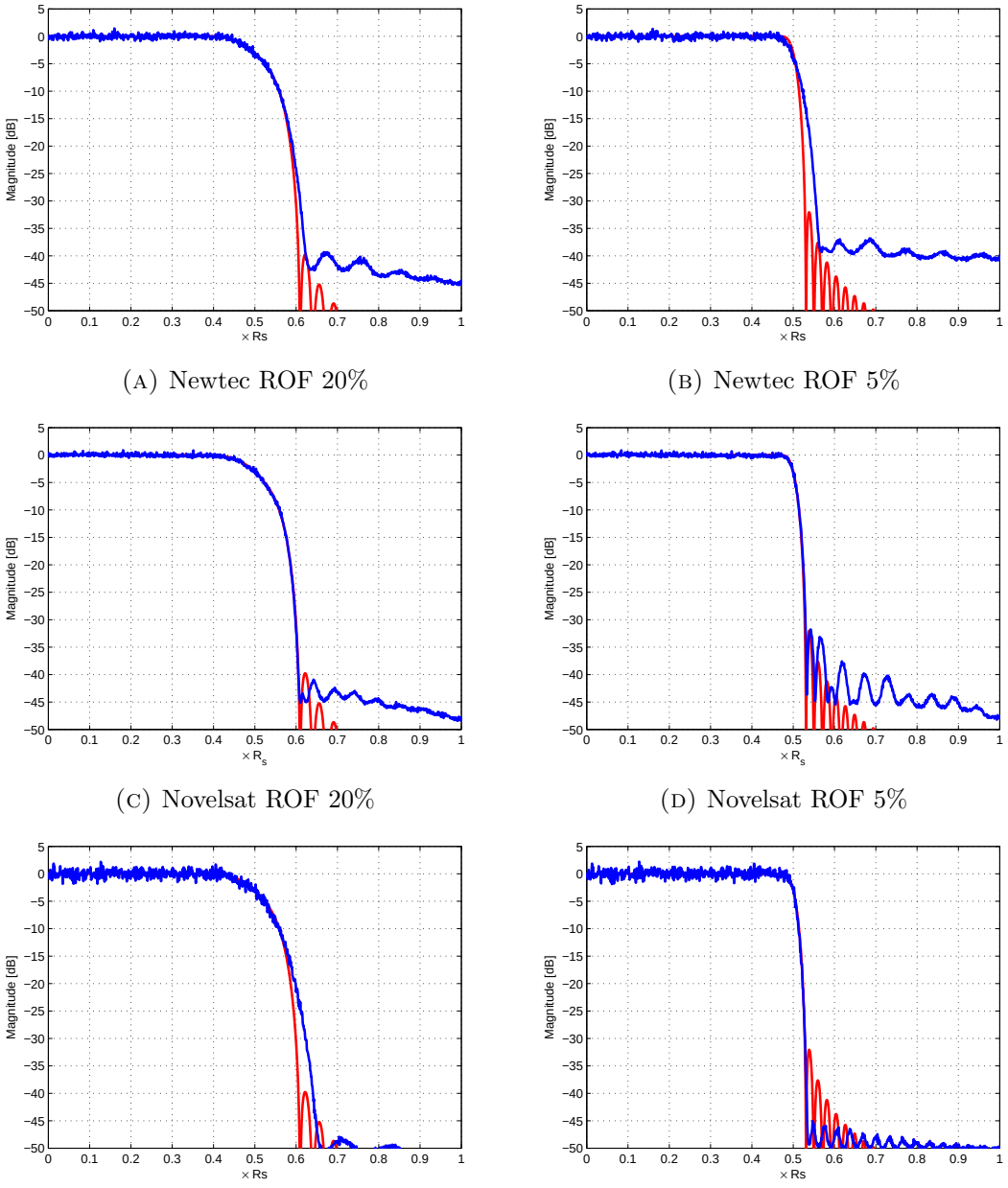

(A) Newtec ROF 20%

(B) Newtec ROF 5%

(C) Novelsat ROF 20%

(D) Novelsat ROF 5%

(E) Workmicrowave ROF 20%

(F) Workmicrowave ROF 5%

FIGURE C.1: SRRC filter shapes used in simulation (red lines) against measured transmit signal spectrum, for different modem manufactures (blue lines)

decreasing the Roll-Off, the number of taps to consider for the FIR filter design increases. For instance, we considered 97 and 161 taps for ROF 20% and 5% respectively, with an interpolation factor of 4. Figure C.1 shows a comparison (for two selected Roll-Offs) between filter shapes designed for simulations against measured transmit signal spectrum for professional modulators of different brands. Now if we take the simulated shapes as a reference, we can notice that in some cases the actual Roll-Off with which the transmit signals are shaped, sensibly deviates from the one declared by the manufacturer. Although we can get a snapshot of the transmit signal spectrum, by hanging a signal

analyser at the modulator output, there is no way to verify the shape of the receive filter at demodulator side, which is however supposed to match the transmit one, but it may also not be the case.

Bibliography

[1] Michel Bousquet Grard Maral. *Satellite Communications Systems, 5th Edition*. 2009.

[2] Koen Willems. Dvb-s2x demystified. Technical report, Newtec, 2014.

[3] Digital Video Broadcasting group. *Second generation framing structure, channel coding and modulation systems for Broadcasting, Interactive Services, News Gathering and other broadband satellite applications. Part II: S2-Extensions (DVB-S2X)*, 2014.

[4] Digital Video Broadcasting group. *ETSI EN 302 307, Second generation framing structure, channel coding and modulation systems for Broadcasting, Interactive Services, News Gathering and other broadband satellite applications (DVB-S2)*. European Telecommunications Standards Institute, 2005.

[5] Digital Video Broadcasting group. *ETSI TR 102 376, User guidelines for the second generation system for Broadcasting, Interactive Services, News Gathering and other broadband satellite applications (DVB-S2)*. European Telecommunications Standards Institute, 2005.

[6] R. De Gaudenzi E. Casini and A. Ginesi. Dvb-s2 modem algorithms design and performance over typical satellite channels. *International Journal of Satellite Communications and Networking*, 2004.

[7] Guido Verfaillie. Improving the transponder utilisation. Technical report, Newtec, 2008.

[8] Guido Verfaillie. Equalising and predistortion: The equalink concept. Technical report, Newtec, 2008.

[9] Giovanni Cherubini Nevio Benvenuto. *Algorithms for Communications Systems and their Application*. 2000.